

University of Strathclyde  
Department of Pure and Applied Chemistry

**Studies in Raman, Infrared and Acoustic Emission  
Spectrometries, and Reaction Calorimetry for  
Process Analysis.**

Pamela Allan

A thesis submitted to the Department of Pure and Applied Chemistry,  
University of Strathclyde, Glasgow, in partial fulfilment for the degree  
of Doctor of Philosophy

2008

**Declaration of author's rights:**

The copyright of this thesis belongs to the author under the terms of the United Kingdom Copyright Acts as qualified by the University of Strathclyde Regulation 3.49. Due to acknowledgement must always be made of the use of any material contained in, or derived from, this thesis.

## **Contents**

### **Contents**

iii

12 Appendix 1 .....	288
12.1 Concentrations and particle size effects in powder blending – monitoring a model process by near infrared spectrometry .....	288
12.1.1 Powder blending (different concentrations and particle sizes) .....	288
12.1.2 Powder blending (constant mass with different particle sizes).....	297
12.2 Conclusions (NIR spectrometry) .....	301
13 Appendix 2.....	302
13.1 Concentration and particle size effects in powder blending – monitoring a model process by Raman spectrometry.....	302
14 Appendix 3.....	306
14.1 Monitoring a model powder blending process by acoustic emission using three different transducers.....	306
14.1.1 Nano 30 transducer .....	306
14.1.2 IS transducer .....	309
14.1.3 WD transducer .....	310
15 Appendix 4.....	312
15.1 NIR monitoring of powder blending.....	312
16 Appendix 5 .....	320
16.1 AE monitoring of powder blending at pilot scale .....	320
17 Appendix 6.....	326
17.1 Preliminary investigation of butanol feed rate .....	326
17.2 Investigation of reactor temperature control.....	330
17.3 Comparison of enthalpy and GC data .....	331
17.4 PC1 and PC2 scores from NIR PCA models .....	332
17.5 PC1 and PC2 scores from MIR PCA models .....	333
17.6 Prediction of butyl acetate concentrations from NIR PLS models .....	334
17.7 Prediction of butyl acetate concentrations from MIR PLS models.....	340

## 12 APPENDIX 1

### 12.1 Concentrations and particle size effects in powder blending – monitoring a model process by near infrared spectrometry

#### 12.1.1 Powder blending (different concentrations and particle sizes)

First derivative signal processing (Savitsky – Golay, 5 point and second order polynomial) was applied to NIR spectra to correct for baseline offset and makes the regions undergoing change more obvious. The first derivative spectra for different masses of aspirin added to Avicel are illustrated in Figure 181. The first derivative spectra clearly shows an increase in aspirin concentration leads to an increase in the NIR signal at 1116 nm and 1643 nm.

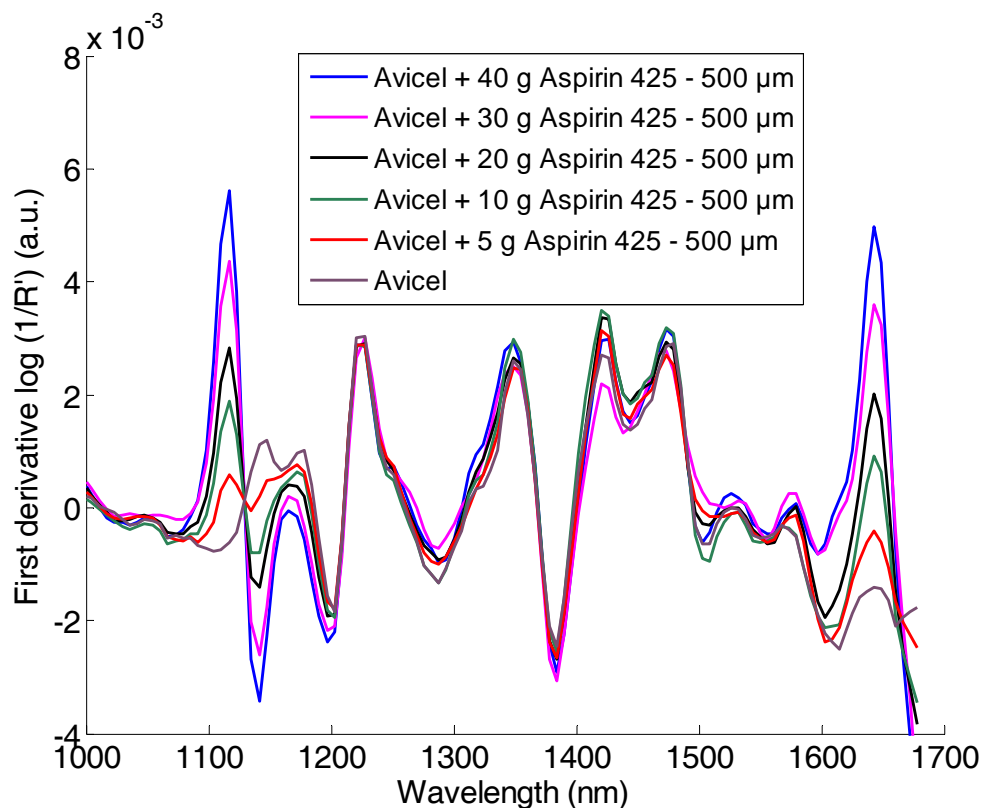


**Figure 181.** First derivative log  $1/R'$  NIR spectra at 800 s of increasing masses of aspirin (particle size 425 – 500  $\mu\text{m}$ ) added to Avicel, mixing at impeller speed 50 rpm.

Mixing profiles were produced by plotting the first derivative aspirin peak intensity at 1643.2 nm for each addition of aspirin of particle size ranges 425 – 500, 250 – 300 and < 106  $\mu\text{m}$ , shown in Figure 182, Figure 183 and Figure 184, respectively. The mixing profile from the first overtone mirrors data obtained by Bellamy, where increasing masses of aspirin (un-sieved therefore constant particle size) were added to Avicel.<sup>15</sup> A large peak in the mixing profile occurs at approximately 130 s, resulting from the concentration of aspirin moving through the NIR sample volume before a homogeneous mixture is obtained. Furthermore, NIR signals took longer to reach the steady state for increased masses of powder added. Lastly, the magnitude of the signals at steady state increase with increasing mass of aspirin.

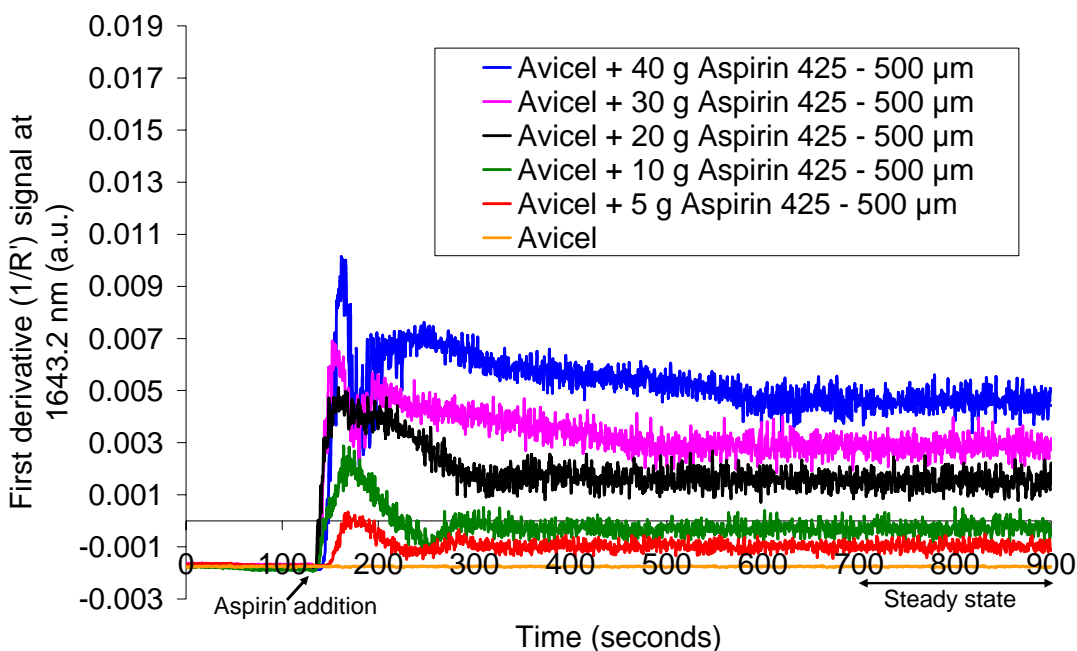


**Figure 182.** NIR mixing profiles of first derivative signals at 1643.2 nm, for mixtures of increasing masses of aspirin (particle size 425 – 500  $\mu\text{m}$ ) with 75 g Avicel PH-101, mixing at 50 rpm.

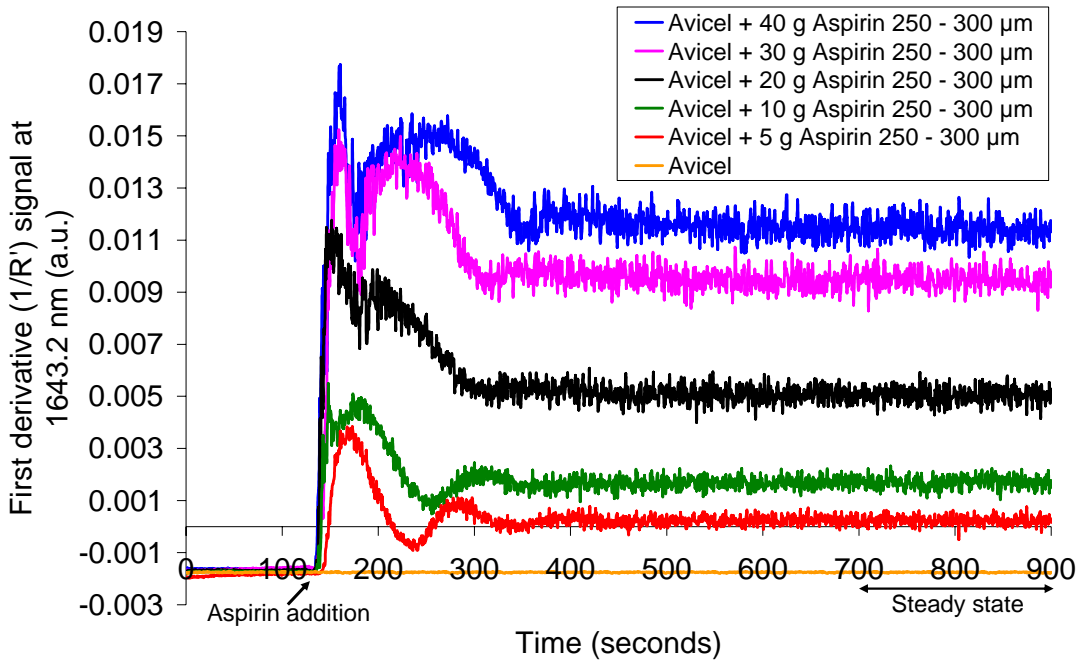


**Figure 183.** NIR mixing profiles of first derivative signals at 1643.2 nm, for mixtures of increasing masses of aspirin (particle size 250 – 300 µm) with 75 g Avicel PH-101, mixing at 50 rpm.

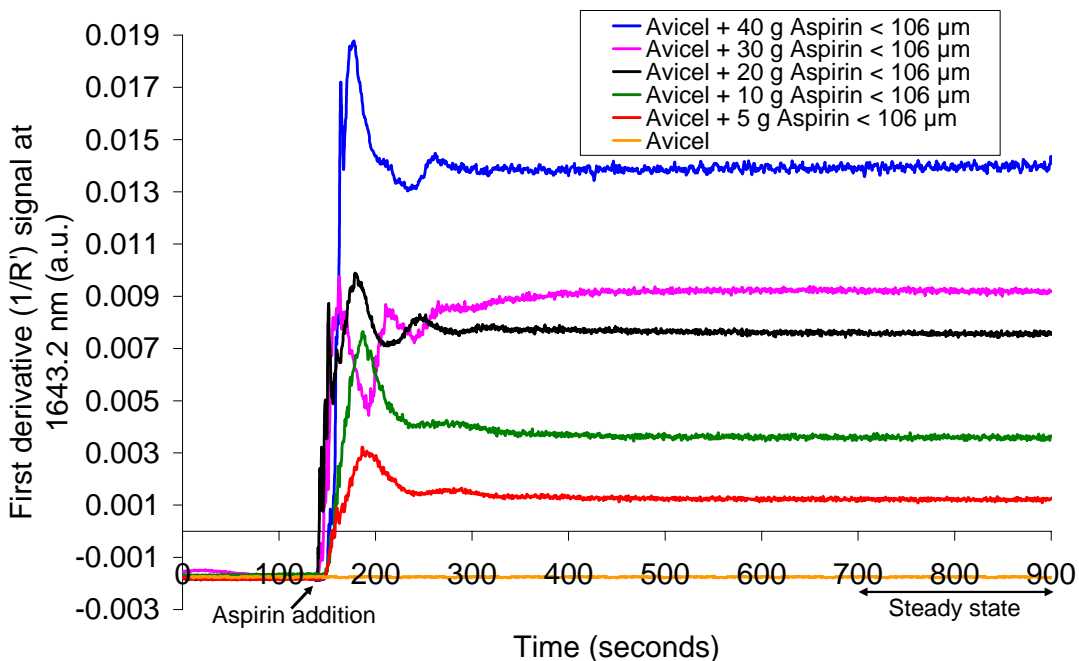


**Figure 184.** NIR mixing profiles of first derivative signals at 1643.2 nm, for mixtures of increasing masses of aspirin (particle size 250 – 300 µm) with 75 g Avicel PH-101, mixing at 50 rpm.

The mean signal, standard deviation, CV and peak-to-peak noise have been calculated from the mixing profiles and are illustrated in Table 39 to Table 44.

**Table 13.** NIR calibration data for 700 to 900 s calculated from signals at 1643.2 nm acquired for the addition of aspirin, particle size 425 – 500 µm, to 75 g Avicel, mixing at impeller speed 50 rpm.

Mixture	Aspirin Conc % w/w	Mean signal (a.u.)	S.D.	CV	Peak min (a.u.)	Peak Max (a.u.)	Noise (a.u.)
75 g Avicel + 40 g Aspirin	53	0.004618	0.000345	7.46	0.003722	0.005466	0.001744
75 g Avicel + 30 g Aspirin	40	0.002870	0.000317	11.05	0.002125	0.003767	0.001641
75 g Avicel + 20 g Aspirin	27	0.001544	0.000331	21.46	0.000839	0.002386	0.001547
75g Avicel + 10 g Aspirin	13	-0.000262	0.000227	-86.66	-0.000796	0.000445	0.001241
75 g Avicel + 5 g Aspirin	7	-0.000967	0.000163	-16.81	-0.001328	-0.000565	0.000763
75 g Aspirin	0	-0.001754	0.000016	-0.89	-0.001795	-0.001716	0.000079

**Table 14.** NIR calibration data for 700 to 900 s calculated from signals at 1116.5 nm acquired for the addition of aspirin, particle size 425 – 500 µm, to 75 g Avicel, mixing at impeller speed 50 rpm.

Mixture	Aspirin Conc % w/w	Mean signal (a.u.)	S.D.	CV	Peak min (a.u.)	Peak Max (a.u.)	Noise (a.u.)
75 g Avicel + 40 g Aspirin	53	0.005743	0.000251	4.38	0.005150	0.006408	0.001258
75 g Avicel + 30 g Aspirin	40	0.004188	0.000235	5.60	0.003598	0.004759	0.001161
75 g Avicel + 20 g Aspirin	27	0.002919	0.000241	8.25	0.002368	0.003542	0.001174
75g Avicel + 10 g Aspirin	13	0.001378	0.000159	11.53	0.001052	0.001845	0.000792
75 g Avicel + 5 g Aspirin	7	0.000518	0.000110	21.25	0.000245	0.000801	0.000556
75 g Aspirin	0	-0.000522	0.000110	-21.00	-0.000731	-0.000488	0.000243

**Table 15.** NIR calibration data for 700 to 900 s calculated from signals at 1643.2 nm acquired for the addition of aspirin, particle size 250 – 300 µm, to 75 g Avicel, mixing at impeller speed 50 rpm.

Mixture	Aspirin Conc % w/w	Mean signal (a.u.)	S.D.	CV	Peak min (a.u.)	Peak Max (a.u.)	Noise (a.u.)
75 g Avicel + 40 g Aspirin	53	0.011427	0.000389	3.41	0.010565	0.012430	0.001864
75 g Avicel + 30 g Aspirin	40	0.009487	0.000343	3.61	0.008480	0.010435	0.001955
75 g Avicel + 20 g Aspirin	27	0.005052	0.000286	5.66	0.004291	0.005729	0.001439
75g Avicel + 10 g Aspirin	13	0.001697	0.000215	12.69	0.001170	0.002216	0.001046
75 g Avicel + 5 g Aspirin	7	0.000237	0.000163	68.58	-0.000237	0.000662	0.000899
75 g Aspirin	0	-0.001754	0.000016	-0.89	-0.001795	-0.001716	0.000079

**Table 16.** NIR calibration data for 700 to 900 s calculated from signals at 1116.5 nm acquired for the addition of aspirin, particle size 250 – 300 µm, to 75 g Avicel, mixing at impeller speed 50 rpm.

Mixture	Aspirin Conc % w/w	Mean signal (a.u.)	S.D.	CV	Peak min (a.u.)	Peak Max (a.u.)	Noise (a.u.)
75 g Avicel + 40 g Aspirin	53	0.006475	0.000133	2.05	0.006157	0.006786	0.000629
75 g Avicel + 30 g Aspirin	40	0.005428	0.000119	2.20	0.005114	0.005705	0.000591
75 g Avicel + 20 g Aspirin	27	0.003635	0.000110	3.02	0.003373	0.003907	0.000535
75g Avicel + 10 g Aspirin	13	0.002017	0.000082	4.07	0.001798	0.002223	0.000425
75 g Avicel + 5 g Aspirin	7	0.000717	0.000055	7.72	0.000553	0.000874	0.000321
75 g Aspirin	0	-0.000522	0.000110	-21.00	-0.000731	-0.000488	0.000243

**Table 17.** NIR calibration data for 700 to 900 s calculated from signals at 1643.2 nm acquired for the addition of aspirin, particle size < 106 µm, to 75 g Avicel, mixing at impeller speed 50 rpm.

Mixture	Aspirin Conc % w/w	Mean signal (a.u.)	S.D.	CV	Peak min (a.u.)	Peak Max (a.u.)	Noise (a.u.)
75 g Avicel + 40 g Aspirin	53	0.013959	0.000110	0.79	0.013688	0.014233	0.000545
75 g Avicel + 30 g Aspirin	40	0.009201	0.000059	0.64	0.009047	0.009326	0.000279
75 g Avicel + 20 g Aspirin	27	0.007569	0.000053	0.70	0.007452	0.007694	0.000242
75g Avicel + 10 g Aspirin	13	0.003591	0.000056	1.56	0.003466	0.003742	0.000276
75 g Avicel + 5 g Aspirin	7	0.001216	0.000039	3.24	0.001107	0.001315	0.000208
75 g Aspirin	0	-0.001754	0.000016	-0.89	-0.001795	-0.001716	0.000079

**Table 18.** NIR calibration data for 700 to 900 s calculated from signals at 1116.5 nm acquired for the addition of aspirin, particle size < 106 µm, to 75 g Avicel, mixing at impeller speed 50 rpm.

Mixture	Aspirin Conc % w/w	Mean signal (a.u.)	S.D.	CV	Peak min (a.u.)	Peak Max (a.u.)	Noise (a.u.)
75 g Avicel + 40 g Aspirin	53	0.005750	0.000028	0.48	0.005683	0.005820	0.000136
75 g Avicel + 30 g Aspirin	40	0.003842	0.000022	0.57	0.003790	0.003894	0.000104
75 g Avicel + 20 g Aspirin	27	0.002658	0.000017	0.65	0.002615	0.002700	0.000086
75g Avicel + 10 g Aspirin	13	0.001876	0.000016	0.83	0.001841	0.001916	0.000075
75 g Avicel + 5 g Aspirin	7	0.000680	0.000013	1.90	0.000647	0.000711	0.000064
75 g Aspirin	0	-0.000522	0.000110	-21.00	-0.000731	-0.000488	0.000243

The average intensity between 700 and 900 s at the steady state was calculated for the first overtone 1643.2 nm and second overtone 1116.5 nm (refer to Figure 185 and Figure 186, respectively). The average first derivative signal for the first and second overtones increased with increasing mass of aspirin at each particle size, to give an approximately linear response for the first overtone and slight curvature for the second overtone. The first overtone (1643.2 nm) illustrates a decrease in signal intensity at each mass of aspirin with increasing particle size.

This trend is also observed in the peak-to-peak noise values calculated for the first (1643.2 nm) and second (1116.5 nm) overtone (see Figure 187 and Figure 188).

The peak-to peak noise of the constant signal in the blending profile for the second overtone peak of aspirin at 1116.5 nm, increased with particle size for each mass of aspirin added to Avicel until a maximum was reached, at approximately 20 g aspirin added to Avicel (see Figure 188). A similar trend was observed by Bellamy.<sup>15</sup> The variation in signal is caused by the aspirin particles moving into and away from the observation region of the NIR spectrometer, this will be much greater for the larger particle size fractions than for the more abundant smaller particle size fractions.

Only the mixing profiles based on the second overtone aspirin peak displayed the trend of increasing peak-to peak noise with particle size. The first overtone signals showed a similar peak-to-peak noise for the medium and large aspirin particle size ranges (particle size 250 – 300  $\mu\text{m}$  and 425 – 500  $\mu\text{m}$ ) in comparison to the small aspirin particle size range, < 106  $\mu\text{m}$  (see Figure 187). However, all three aspirin particle size ranges reached a maximum peak-to peak noise between 20 and 40 g aspirin added to Avicel. Deeper information depths occur at second overtone peaks, therefore a greater volume of sample can be analyzed, which can remove some of the influence from the variation in particle size, through multiple scattering.

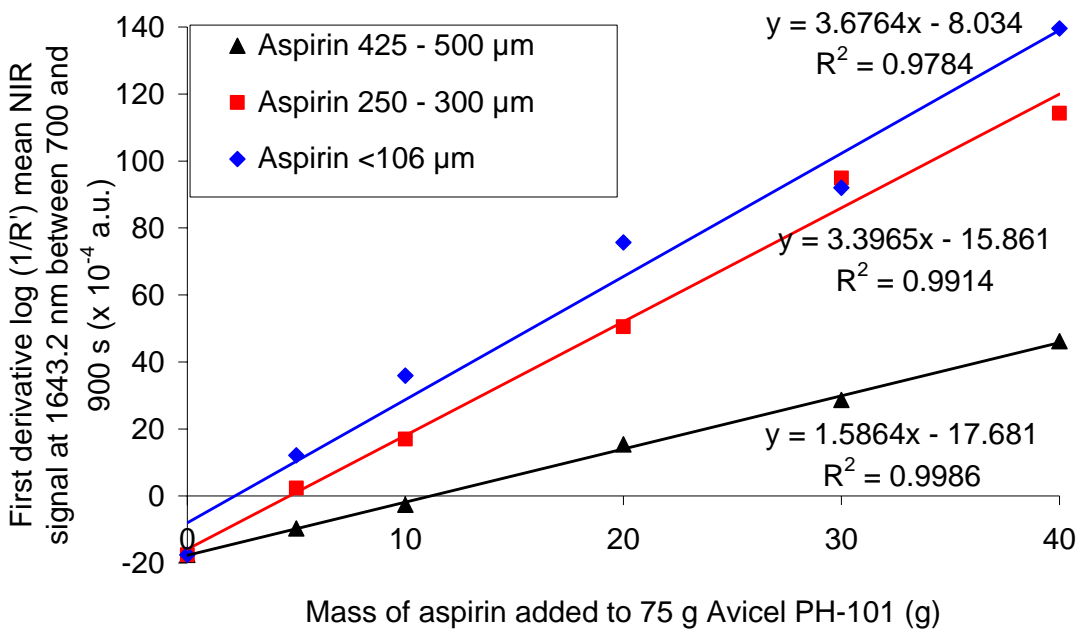


**Figure 185.** Average first derivative log (1/R') at 1643.2 nm between 700 and 900 s for mixtures of aspirin of varying particle size and mass added to 75 g Avicel PH-101, mixing at 50 rpm.

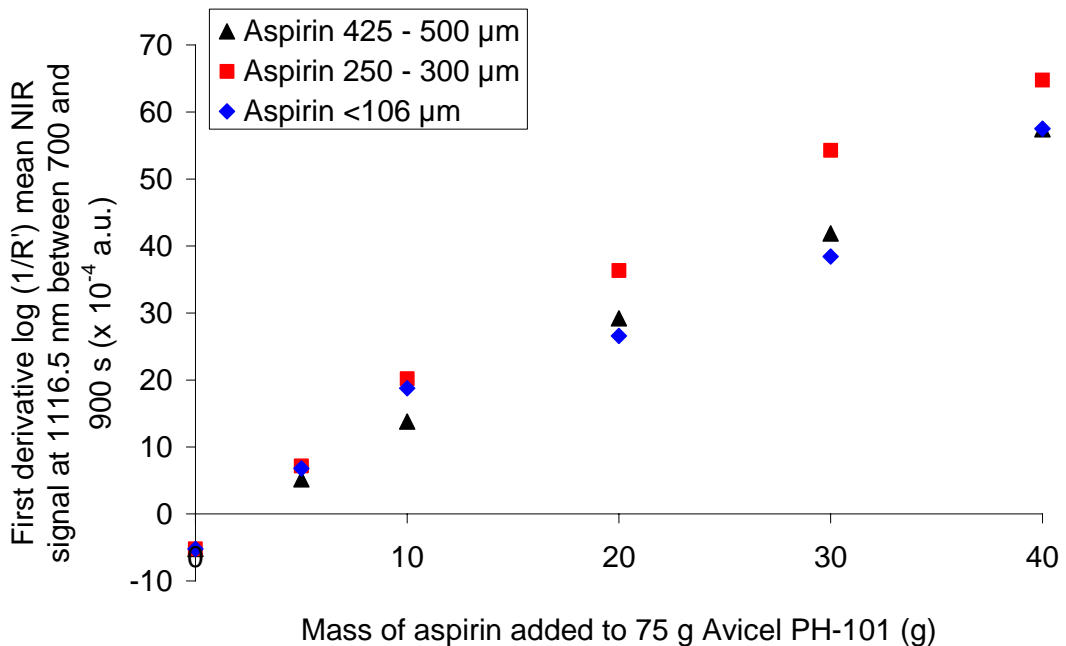


**Figure 186.** Average first derivative log (1/R') at 1116.5 nm between 700 and 900 s for mixtures of aspirin of varying particle size and mass added to 75 g Avicel PH-101, mixing at 50 rpm.

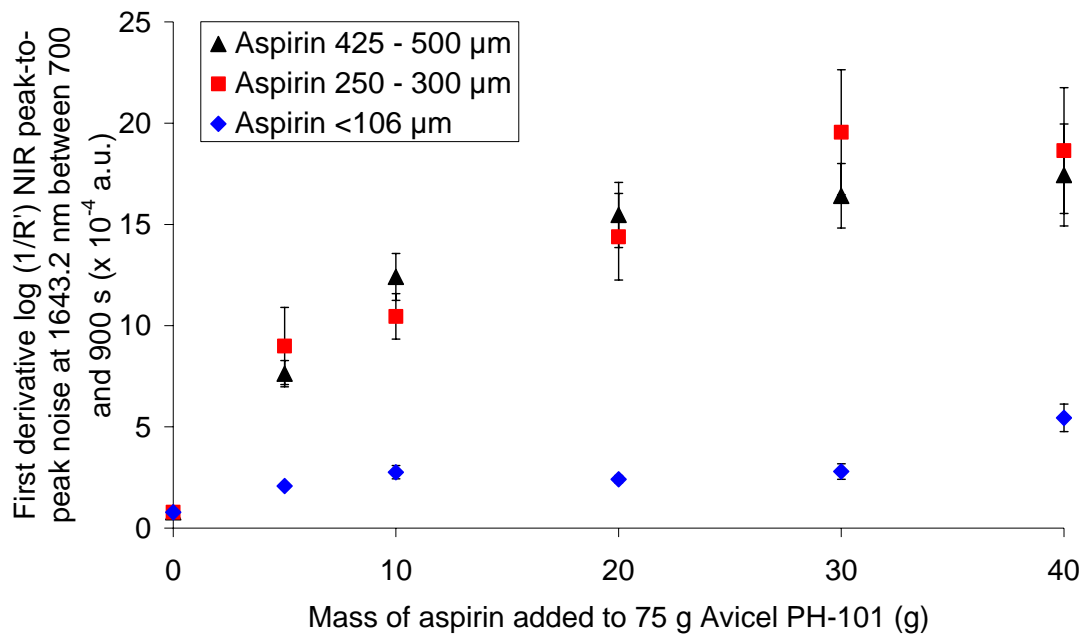


**Figure 187.** NIR peak-to-peak noise plots acquired for the additions of different particle sizes and mass of aspirin to 75 g of Avicel PH-101 between 700 and 900 s (in 50 s intervals) at first derivative log (1/R') signal 1643.2 nm. Each point is the mean of 4 values  $\pm$  one standard deviation.

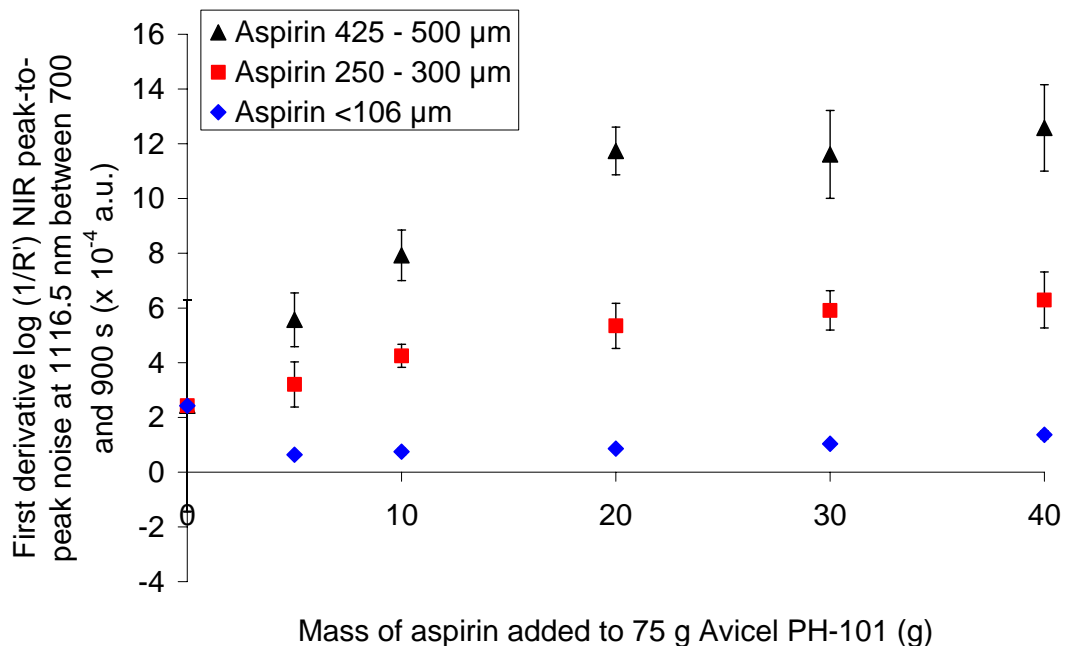


**Figure 188.** NIR peak-to-peak noise plots acquired for the additions of different particle sizes and mass of aspirin to 75 g of Avicel PH-101 between 700 and 900 s (in 50 s intervals) at first derivative log (1/R') signal 1116.5 nm. Each point is the mean of 4 values  $\pm$  one standard deviation.

### 12.1.2 Powder blending (constant mass with different particle sizes)

First derivative signal processing (Savitsky – Golay, 5 point and second order polynomial) was applied to NIR spectra to correct for baseline offset and makes the regions undergoing change more obvious. The first derivative spectra of a constant mass of aspirin with increasing particle sizes added to Avicel are illustrated in Figure 189 and the mixing profile over the mixing period are shown in Figure 190.

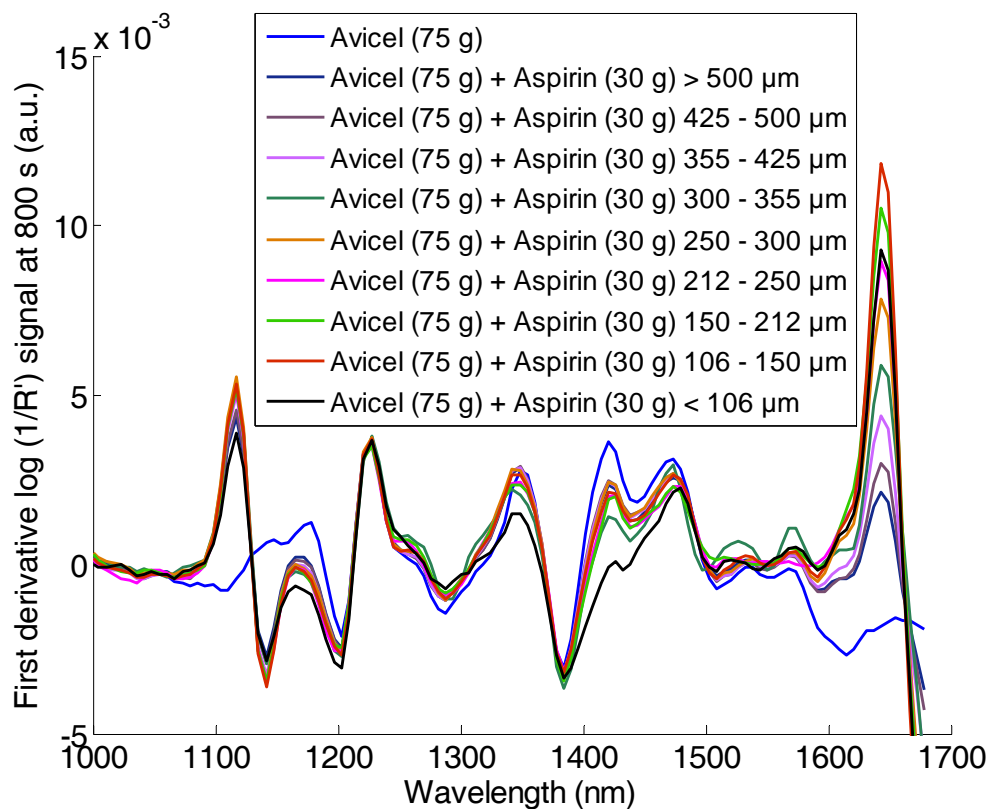


**Figure 189.** First derivative log  $1/R'$  NIR spectra at 800 s of constant mass of aspirin with increasing particle sizes added to Avicel, mixing at impeller speed 50 rpm.

Mixing profiles were produced for aspirin peaks at 1643.2 nm for each addition of aspirin, Figure 190. The mixing profile from the first overtone mirrors data obtained by Bellamy et al.<sup>15</sup> Only this investigation has used 30 g of aspirin in comparison to 7.5 g added previously. Therefore, signals obtained in this investigation are at slightly higher intensity. A large peak in the mixing profile occurs at approximately 130 s, resulting from the concentration of aspirin moving through the NIR sample volume before a homogeneous mixture is obtained, although particles in the size

range  $< 106 \mu\text{m}$  do not fit this trend. The magnitudes of the signals at steady state are larger with increasing particle size.

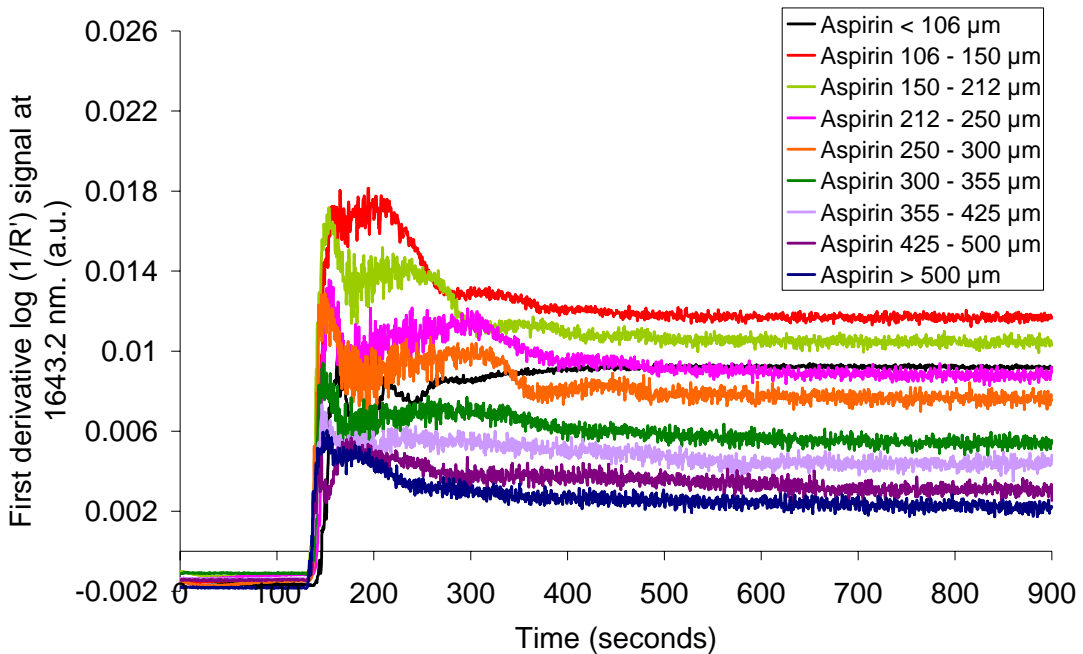


**Figure 190. NIR mixing profiles of first derivative signals at 1643.2 nm, for mixtures of 30 g aspirin of varying particle size with 75 g Avicel PH-101, mixing at 50 rpm.**

The mean signal, standard deviation, CV and peak-to-peak noise been calculated from the mixing profiles and are illustrated in Table 19 and Table 20.

**Table 19.** NIR calibration data calculated from signals acquired for the addition of 30 g of aspirin, of varying particle sizes, to 75 g Avicel between 700 and 900 seconds at 1643.2 nm, mixing at impeller speed 50 rpm.

Aspirin particle size ( $\mu\text{m}$ )	Mean signal (a.u.)	S.D.	CV	Peak min (a.u.)	Peak Max (a.u.)	Noise (a.u.)
500	0.002252	0.000191	8.50	0.001748	0.002685	0.000937
462.5	0.003087	0.000204	6.60	0.002524	0.003636	0.001112
390	0.004385	0.000222	5.05	0.003766	0.004914	0.001148
327.5	0.005434	0.000199	3.66	0.004922	0.005923	0.001001
275	0.007645	0.000210	2.74	0.007093	0.008209	0.001116
231	0.008815	0.000178	2.02	0.008397	0.009292	0.000895
181	0.010461	0.000163	1.56	0.010018	0.010861	0.000843
128	0.011678	0.000131	1.12	0.011318	0.011992	0.000674
<106	0.009201	0.000059	0.64	0.009047	0.009326	0.000279

**Table 20.** NIR calibration data calculated from signals acquired for the addition of 30 g of aspirin, of varying particle sizes, to 75 g Avicel between 700 and 900 seconds at 1116.5 nm, mixing at impeller speed 50 rpm.

Aspirin particle size ( $\mu\text{m}$ )	Mean signal (a.u.)	S.D.	CV	Peak min (a.u.)	Peak Max (a.u.)	Noise (a.u.)
500	0.004538	0.000184	4.06	0.004085	0.004937	0.000852
462.5	0.004709	0.000157	3.34	0.004285	0.005143	0.000858
390	0.005015	0.000144	2.88	0.004589	0.005397	0.000808
327.5	0.005156	0.000099	1.91	0.004909	0.005387	0.000478
275	0.005418	0.000088	1.62	0.005190	0.005645	0.000455
231	0.005118	0.000061	1.20	0.004970	0.005279	0.000309
181	0.005145	0.000048	0.94	0.005017	0.005259	0.000242
128	0.005285	0.000032	0.60	0.005203	0.005364	0.000161
<106	0.003842	0.000022	0.57	0.003790	0.003894	0.000104

The average intensity between 700 and 900 s at the steady state was calculated for the first overtone 1643.2 nm and the second overtone 1116.5 nm, Figure 191. The average first derivative signal for the first overtone increases initially (for < 106  $\mu\text{m}$  to 106 – 150  $\mu\text{m}$ ) then decreases with increasing particle size. In contrast, the second overtone shows little effect of particle size, with only an initial increase in signal for < 106  $\mu\text{m}$  to 106 – 150  $\mu\text{m}$ . In a similar study by Bellamy et al.<sup>15</sup> the same trends were observed. However, the particles investigated were larger than the wavelength of the incident radiation across the entire region, so it would be expected that signals should increase with increasing aspirin particle size. In separate studies by Gupta et al.<sup>239</sup> and Barajas et al.<sup>95</sup> the NIR signal was found to increase for increasing particle sizes of static powders. The decrease in signal intensity with increasing particle size may be due to a reduction in the number of reflections or scattering events involving the minority component.

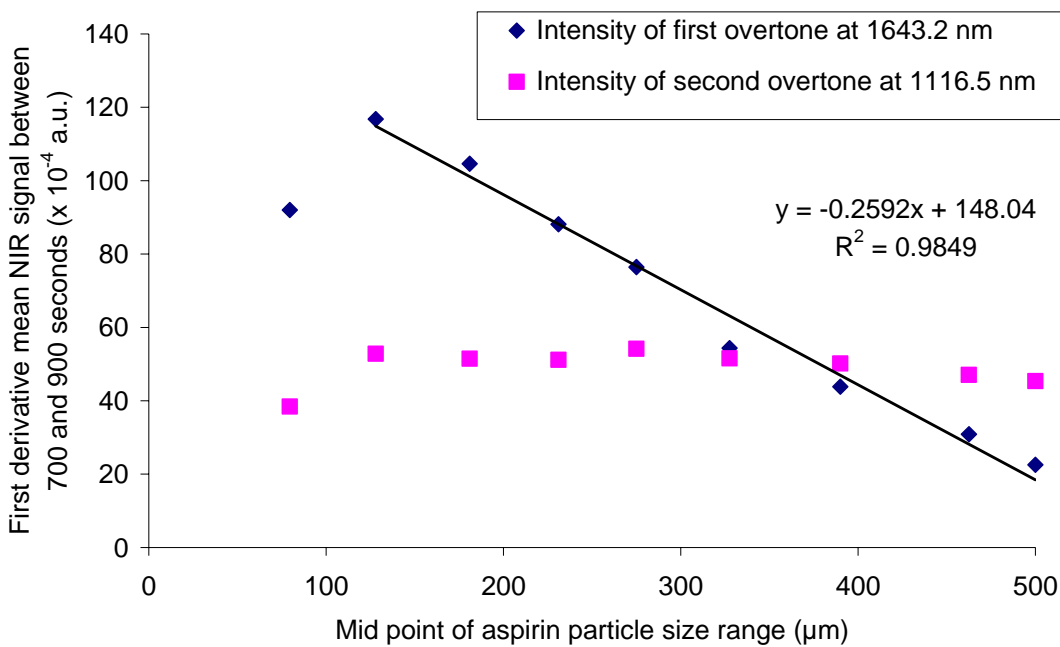


**Figure 191.** Average first derivative log (1/R') at 1643.2 and 1116.5 nm between 700 and 900 seconds for mixtures of 30 g aspirin of varying particle size and 75 g Avicel PH-101, mixing at 50 rpm.

The peak-to-peak noise of the mixing profile signal between 700 and 900 s was calculated for the first overtone (1643.2 nm) and the second overtone (1116.5 nm) and was found to generally increase with increasing particle size.

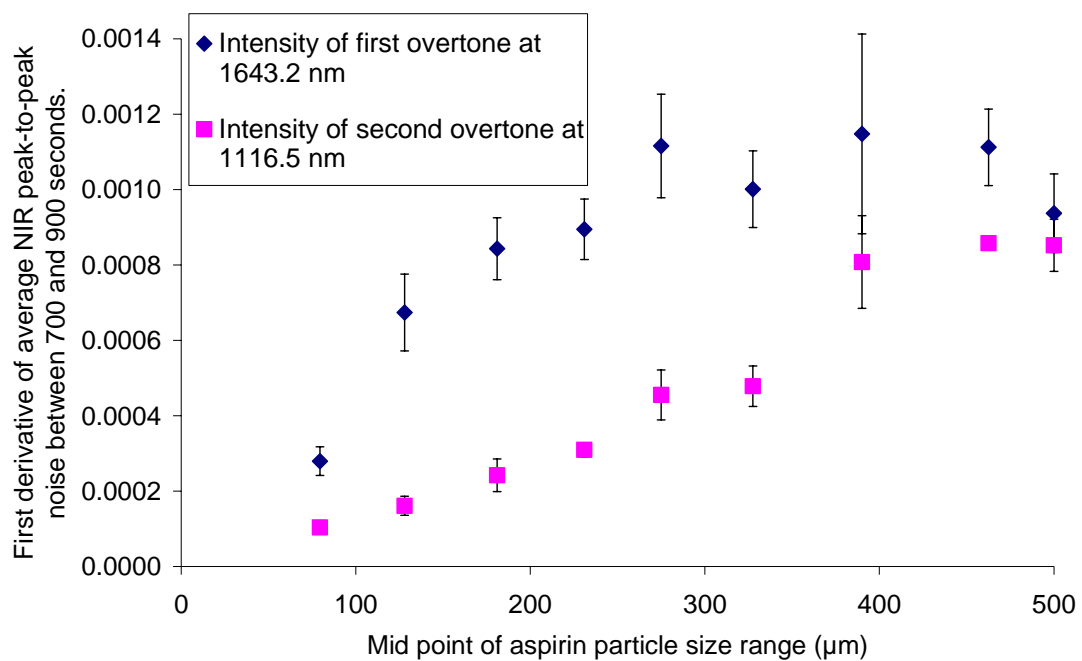


**Figure 192.** NIR plots of the peak-to-peak noise intensities for aspirin at 1643.2 and 1116.5 nm between 700 and 900 s (in 50 s intervals) after the additions of different particle sizes aspirin (30 g) to 75 g Avicel PH-101. Each point is the mean of 4 values  $\pm$  one standard deviation.

## 12.2 Conclusions (NIR spectrometry)

The NIR spectrum produced when monitoring powder mixing is sensitive to both the mass and particle size of the powders. With the first overtone peaks being much more sensitive to particle size than the second overtone peak. The first overtone peak decreased in signal intensity as the particle size increased, to give an approximately linear response, with the exception of the smallest particle size  $< 106 \mu\text{m}$ . However the second overtone peak remained fairly constant. This trend occurs as a result of the second overtone signals having a greater information depth. An increase in both the first and second overtones is observed with an increase in mass of the secondary component, and an approximately linear response was obtained.

## 13 APPENDIX 2

### 13.1 Concentration and particle size effects in powder blending – monitoring a model process by Raman spectrometry

**Table 21.** Raman PhAT probe calibration data for 700 – 900 s calculated from signals at  $1606.4\text{ cm}^{-1}$  acquired for the addition of different masses of aspirin, particle size 425 – 500  $\mu\text{m}$ , to 75 g Avicel PH-101, mixing at impeller speed 50 rpm.

Mixture	Aspirin Conc % w/w	Mean signal (a.u.)	S.D.	CV	Peak min (a.u.)	Peak Max (a.u.)	Noise (a.u.)
75 g Avicel	0	-0.01	0.10	-832.16	-0.18	0.15	0.33
75 g Avicel + 40 g Aspirin	35	-12.46	0.35	-2.80	-13.01	-11.93	1.08
75 g Avicel + 30 g Aspirin	29	-9.77	0.35	-3.61	-10.29	-9.26	1.03
75 g Avicel + 20 g Aspirin	21	-6.84	0.36	-5.28	-7.32	-6.30	1.02
75g Avicel + 10 g Aspirin	12	-3.44	0.25	-7.36	-3.85	-2.95	0.90
75 g Avicel + 5 g Aspirin	6	-1.85	0.16	-8.67	-2.11	-1.60	0.51

**Table 22.** Raman PhAT probe calibration data for 700 – 900 s calculated from signals at  $751.2\text{ cm}^{-1}$  acquired for the addition of different masses of aspirin, particle size 425 – 500  $\mu\text{m}$ , to 75 g Avicel PH-101, mixing at impeller speed 50 rpm.

Mixture	Aspirin Conc % w/w	Mean signal (a.u.)	S.D.	CV	Peak min (a.u.)	Peak Max (a.u.)	Noise (a.u.)
75 g Avicel	0	-0.01	0.12	-1412.90	-0.17	0.20	0.37
75 g Avicel + 40 g Aspirin	35	-7.65	0.22	-2.86	-8.08	-7.25	0.82
75 g Avicel + 30 g Aspirin	29	-5.97	0.19	-3.24	-6.23	-5.67	0.56
75 g Avicel + 20 g Aspirin	21	-4.16	0.23	-5.55	-4.53	-3.81	0.72
75g Avicel + 10 g Aspirin	12	-2.08	0.17	-8.15	-2.38	-1.84	0.54
75 g Avicel + 5 g Aspirin	6	-1.10	0.14	-12.57	-1.32	-0.91	0.41

**Table 23.** Raman PhAT probe calibration data for 700 – 900 s calculated from signals at  $1606.4\text{ cm}^{-1}$  acquired for the addition of different masses of aspirin, particle size 250 – 300  $\mu\text{m}$ , to 75 g Avicel PH-101, mixing at impeller speed 50 rpm.

Mixture	Aspirin Conc % w/w	Mean signal (a.u.)	S.D.	CV	Peak min (a.u.)	Peak Max (a.u.)	Noise (a.u.)
75 g Avicel	0	-0.01	0.10	-832.16	-0.18	0.15	0.33
75 g Avicel + 40 g Aspirin	35	-13.22	0.20	-1.48	-13.57	-12.89	0.68
75 g Avicel + 30 g Aspirin	29	-10.29	0.22	-2.19	-10.59	-9.90	0.69
75 g Avicel + 20 g Aspirin	21	-7.12	0.19	-2.63	-7.42	-6.86	0.56
75g Avicel + 10 g Aspirin	12	-3.78	0.15	-4.04	-4.02	-3.56	0.46
75 g Avicel + 5 g Aspirin	6	-1.96	0.12	-6.27	-2.13	-1.77	0.37

**Table 24.** Raman PhAT probe calibration data for 700 – 900 s calculated from signals at  $751.2\text{ cm}^{-1}$  acquired for the addition of different masses of aspirin, particle size 250 – 300  $\mu\text{m}$ , to 75 g Avicel PH-101, mixing at impeller speed 50 rpm.

Mixture	Aspirin Conc % w/w	Mean signal (a.u.)	S.D.	CV	Peak min (a.u.)	Peak Max (a.u.)	Noise (a.u.)
75 g Avicel	0	-0.01	0.12	-1412.90	-0.17	0.20	0.37
75 g Avicel + 40 g Aspirin	35	-8.02	0.15	-1.87	-8.21	-7.77	0.44
75 g Avicel + 30 g Aspirin	29	-6.27	0.18	-2.87	-6.57	-5.97	0.59
75 g Avicel + 20 g Aspirin	21	-4.31	0.13	-3.05	-4.56	-4.11	0.44
75g Avicel + 10 g Aspirin	12	-2.26	0.13	-5.88	-2.45	-2.05	0.40
75 g Avicel + 5 g Aspirin	6	-1.19	0.11	-9.31	-1.34	-1.00	0.34

**Table 25.** Raman PhAT probe calibration data for 700 – 900 s calculated from signals at 1606.4 cm<sup>-1</sup> acquired for the addition of different masses of aspirin, particle size < 106 µm, to 75 g Avicel PH-101, mixing at impeller speed 50 rpm.

Mixture	Aspirin Conc % w/w	Mean signal (a.u.)	S.D.	CV	Peak min (a.u.)	Peak Max (a.u.)	Noise (a.u.)
75 g Aspirin	0	-0.01	0.10	-832.16	-0.18	0.15	0.33
75 g Avicel + 40 g Aspirin	35	-11.90	0.14	-1.15	-12.12	-11.71	0.41
75 g Avicel + 30 g Aspirin	29	-7.80	0.14	-1.80	-8.00	-7.54	0.47
75 g Avicel + 20 g Aspirin	21	-5.74	0.13	-2.19	-5.97	-5.57	0.40
75g Avicel + 10 g Aspirin	12	-3.57	0.13	-3.74	-3.79	-3.36	0.42
75 g Avicel + 5 g Aspirin	6	-1.76	0.11	-6.43	-1.94	-1.57	0.37

**Table 26.** Raman PhAT probe calibration data for 700 – 900 s calculated from signals at 751.2 cm<sup>-1</sup> acquired for the addition of different masses of aspirin, particle size < 106 µm, to 75 g Avicel PH-101, mixing at impeller speed 50 rpm.

Mixture	Aspirin Conc % w/w	Mean signal (a.u.)	S.D.	CV	Peak min (a.u.)	Peak Max (a.u.)	Noise (a.u.)
75 g Avicel	0	-0.01	0.12	-1412.90	-0.17	0.20	0.37
75 g Avicel + 40 g Aspirin	35	-7.18	0.11	-1.59	-7.37	-7.03	0.34
75 g Avicel + 30 g Aspirin	29	-4.76	0.11	-2.38	-4.94	-4.58	0.37
75 g Avicel + 20 g Aspirin	21	-3.51	0.09	-2.46	-3.65	-3.37	0.28
75g Avicel + 10 g Aspirin	12	-2.15	0.10	-4.80	-2.34	-2.00	0.34
75 g Avicel + 5 g Aspirin	6	-1.06	0.11	-10.19	-1.20	-0.86	0.34

**Table 27.** Raman PhAT probe calibration data calculated from signals acquired for the addition of 30 g of aspirin, of varying particle sizes, to 75 g Avicel PH-101 between 700 and 900 s at  $1606.4\text{ cm}^{-1}$ , mixing at impeller speed 50 rpm.

Particle Size of Aspirin	Aspirin Conc % w/w	Mean signal (a.u)	S.D.	CV	Peak min (a.u.)	Peak Max (a.u.)	Noise (a.u.)
No Aspirin present	0	-0.04	0.12	-303.36	-0.21	0.18	0.39
> 500 $\mu\text{m}$	29	-10.00	0.40	-4.01	-10.55	-9.39	1.16
425 - 500 $\mu\text{m}$	29	-9.97	0.26	-2.65	-10.38	-9.59	0.79
355 - 425 $\mu\text{m}$	29	-10.25	0.22	-2.11	-10.51	-9.93	0.58
300 - 355 $\mu\text{m}$	29	-10.22	0.23	-2.30	-10.62	-9.83	0.80
250 - 300 $\mu\text{m}$	29	-10.20	0.20	-1.97	-10.66	-9.90	0.76
212 - 250 $\mu\text{m}$	29	-10.25	0.18	-1.80	-10.49	-9.95	0.53
150 - 212 $\mu\text{m}$	29	-10.16	0.16	-1.58	-10.42	-9.93	0.49
106 - 150 $\mu\text{m}$	29	-10.01	0.15	-1.48	-10.30	-9.80	0.49
<106 $\mu\text{m}$	29	-7.80	0.14	-1.81	-8.01	-7.54	0.47

**Table 28.** Raman PhAT probe calibration data calculated from signals acquired for the addition of 30 g of aspirin, of varying particle sizes, to 75 g Avicel PH-101 between 700 and 900 s at  $751.2\text{ cm}^{-1}$ , mixing at impeller speed 50 rpm.

Particle Size of Aspirin	Aspirin % w/w	Mean signal (a.u)	S.D.	CV	Peak min (a.u.)	Peak Max (a.u.)	Noise (a.u.)
No Aspirin present	0	-0.02	0.12	-714.88	-0.20	0.20	0.40
> 500 $\mu\text{m}$	29	-6.18	0.25	-4.05	-6.56	-5.81	0.75
425 - 500 $\mu\text{m}$	29	-6.10	0.20	-3.27	-6.43	-5.82	0.61
355 - 425 $\mu\text{m}$	29	-6.28	0.15	-2.38	-6.52	-6.04	0.48
300 - 355 $\mu\text{m}$	29	-6.23	0.16	-2.51	-6.50	-5.93	0.57
250 - 300 $\mu\text{m}$	29	-6.22	0.15	-2.48	-6.48	-5.98	0.50
212 - 250 $\mu\text{m}$	29	-6.21	0.11	-1.73	-6.40	-6.09	0.31
150 - 212 $\mu\text{m}$	29	-6.20	0.11	-1.70	-6.36	-6.04	0.32
106 - 150 $\mu\text{m}$	29	-6.09	0.09	-1.52	-6.22	-5.95	0.27
<106 $\mu\text{m}$	29	-4.76	0.11	-2.37	-4.95	-4.58	0.37

## 14 APPENDIX 3

### 14.1 Monitoring a model powder blending process by acoustic emission using three different transducers

#### 14.1.1 Nano 30 transducer

**Table 29.** AE calibration data calculated from area signals between 2 to 400 kHz at 700 - 900 s after the addition of different masses of aspirin, particle size 425 - 500 µm, to 75 g Avicel PH-101; mixing at impeller speed 50 rpm. AE signals acquired using the Nano 30 transducer.

Mixture	Aspirin Conc % w/w	Mean signal (a.u.)	S.D.	CV	Peak min (a.u.)	Peak Max (a.u.)	Noise (a.u.)
75 g Avicel	0	5.94	0.64	10.79	4.84	8.21	3.37
75 g Avicel + 40 g Aspirin	35	21.09	2.97	14.10	14.38	26.90	12.51
75 g Avicel + 30 g Aspirin	29	15.21	2.37	15.59	10.93	21.89	10.96
75 g Avicel + 20 g Aspirin	21	9.44	1.39	14.68	6.85	12.80	5.95
75g Avicel + 10 g Aspirin	12	9.27	1.29	13.95	6.68	12.95	6.26
75 g Avicel + 5 g Aspirin	6	7.87	1.09	13.87	5.89	11.24	5.35

**Table 30.** AE calibration data calculated from area signals between 2 to 400 kHz at 700 - 900 s after the addition of different masses of aspirin, particle size 250 - 300 µm, to 75 g Avicel PH-101; mixing at impeller speed 50 rpm. AE signals acquired using the Nano 30 transducer.

Mixture	Aspirin Conc % w/w	Mean signal (a.u.)	S.D.	CV	Peak min (a.u.)	Peak Max (a.u.)	Noise (a.u.)
75 g Avicel	0	5.24	0.74	14.21	3.80	7.30	3.50
75 g Avicel + 40 g Aspirin	35	13.73	2.22	16.18	6.98	19.65	12.66
75 g Avicel + 30 g Aspirin	29	11.03	1.67	15.13	6.81	15.42	8.61
75 g Avicel + 20 g Aspirin	21	10.68	1.58	14.82	6.93	15.43	8.50
75g Avicel + 10 g Aspirin	12	8.37	1.04	12.37	6.52	11.66	5.15
75 g Avicel + 5 g Aspirin	6	6.82	0.90	13.23	5.02	10.33	5.32

**Table 31.** AE calibration data calculated from area signals between 2 to 400 kHz at 700 - 900 s after the addition of different masses of aspirin, particle size < 106 µm, to 75 g Avicel PH-101; mixing at impeller speed 50 rpm. AE signals acquired using the Nano 30 transducer.

Mixture	Aspirin Conc % w/w	Mean signal (a.u.)	S.D.	CV	Peak min (a.u.)	Peak Max (a.u.)	Noise (a.u.)
75 g Avicel	0	4.94	0.64	12.97	3.84	7.21	3.37
75 g Avicel + 40 g Aspirin	35	7.14	1.20	16.80	4.53	10.73	6.19
75 g Avicel + 30 g Aspirin	29	15.09	1.45	9.59	12.24	18.46	6.22
75 g Avicel + 20 g Aspirin	21	19.55	1.90	9.73	15.62	23.95	8.33
75g Avicel + 10 g Aspirin	12	7.90	1.01	12.77	5.29	11.10	5.81
75 g Avicel + 5 g Aspirin	6	8.21	0.86	10.42	6.68	10.28	3.60

**Table 32.** AE calibration data calculated from area signals between 2 to 400 kHz at 700 - 900 s after the addition of different particle sizes of aspirin, mass 30 g, to 75 g Avicel PH-101; mixing at impeller speed 50 rpm. AE signals acquired using the Nano 30 transducer.

<b>Particle Size of Aspirin</b>	<b>Aspirin Conc % w/w</b>	<b>Mean signal (a.u.)</b>	<b>S.D.</b>	<b>CV</b>	<b>Peak min (a.u.)</b>	<b>Peak Max (a.u.)</b>	<b>Noise (a.u.)</b>
No Aspirin present	0	5.20	0.61	11.74	3.92	7.69	3.77
> 500 µm	29	17.83	2.29	12.82	13.26	25.94	12.69
425 - 500 µm	29	15.17	1.98	13.04	11.37	20.46	9.09
355 - 425 µm	29	16.79	2.28	13.60	13.01	22.82	9.80
300 - 355 µm	29	16.95	2.30	13.55	13.38	22.70	9.31
250 - 300 µm	29	17.24	2.24	12.97	12.31	24.20	11.89
212 - 250 µm	29	15.65	1.97	12.62	11.72	20.94	9.22
150 - 212 µm	29	13.67	1.75	12.81	10.40	18.94	8.55
106 - 150 µm	29	10.54	1.27	12.10	8.17	14.53	6.36
< 106 µm	29	14.09	1.45	10.27	11.24	17.46	6.22

#### 14.1.2 IS transducer

**Table 33.** AE calibration data calculated from area signals between 14 to 300 kHz, over 200 s from when the AE signal reached a constant value after the addition of different masses of aspirin, particle size < 106 µm, to 75 g Avicel PH-101; mixing at impeller speed 50 rpm. AE signals acquired with the IS transducer.

Mixture	Aspirin Conc % w/w	Mean signal (a.u.)	S.D.	CV	Peak min (a.u.)	Peak Max (a.u.)	Noise (a.u.)
75 g Avicel + 40 g Aspirin	35	0.001688	0.000408	24.17	0.001003	0.003084	0.002081
75 g Avicel + 30 g Aspirin	29	0.001465	0.000378	25.79	0.000948	0.002965	0.002017
75 g Avicel + 20 g Aspirin	21	0.001215	0.000351	28.91	0.000729	0.002659	0.001929
75g Avicel + 10 g Aspirin	12	0.000985	0.000224	22.79	0.000636	0.001639	0.001004
75 g Avicel + 5 g Aspirin	6	0.000889	0.000215	24.19	0.000595	0.001468	0.000873
75 g Avicel	0	0.000906	0.000254	28.02	0.000618	0.001497	0.000879

**Table 34.** AE calibration data calculated from area signals between 14 to 300 kHz, over 200 s from when the AE signal reached a constant value after the addition of different masses of aspirin, particle size 250 - 300 µm, to 75 g Avicel PH-101; mixing at impeller speed 50 rpm. AE signals acquired with the IS transducer.

Mixture	Aspirin Conc % w/w	Mean signal (a.u.)	S.D.	CV	Peak min (a.u.)	Peak Max (a.u.)	Noise (a.u.)
75 g Avicel + 40 g Aspirin	35	0.003068	0.000814	26.52	0.001876	0.006368	0.004492
75 g Avicel + 30 g Aspirin	29	0.001914	0.000562	29.39	0.001085	0.003805	0.002720
75 g Avicel + 20 g Aspirin	21	0.001346	0.000312	23.17	0.000865	0.002278	0.001413
75g Avicel + 10 g Aspirin	12	0.001013	0.000231	22.85	0.000754	0.001702	0.000948
75 g Avicel + 5 g Aspirin	6	0.000850	0.000198	23.31	0.000539	0.001380	0.000840
75 g Avicel	0	0.000711	0.000156	21.94	0.000431	0.001203	0.000772

**Table 35.** AE calibration data calculated from area signals between 14 to 300 kHz, over 200 s from when the AE signal reached a constant value after the addition of different masses of aspirin, particle size 425 – 500 µm, to 75 g Avicel PH-101; mixing at impeller speed 50 rpm. AE signals acquired with the IS transducer.

Mixture	Aspirin Conc % w/w	Mean signal (a.u.)	S.D.	CV	Peak min (a.u.)	Peak Max (a.u.)	Noise (a.u.)
75 g Avicel + 40 g Aspirin	35	0.003756	0.000986	26.26	0.002477	0.006437	0.003961
75 g Avicel + 30 g Aspirin	29	0.002092	0.000556	26.58	0.001325	0.003893	0.002568
75 g Avicel + 20 g Aspirin	21	0.001300	0.000318	24.47	0.000878	0.002176	0.001298
75g Avicel + 10 g Aspirin	12	0.001000	0.000211	21.14	0.000715	0.001563	0.000847
75 g Avicel + 5 g Aspirin	6	0.000842	0.000189	22.47	0.000499	0.001429	0.000930
75 g Avicel	0	0.000739	0.000147	19.84	0.000530	0.001149	0.000619

#### 14.1.3 WD transducer

**Table 36.** AE calibration data calculated from area signals between 10 to 300 kHz, over 200 s from when the AE signal reached a constant value after the addition of different masses of aspirin, particle size < 106 µm, to 75 g Avicel; mixing at impeller speed 50 rpm. AE signals acquired with the WD transducer.

Mixture	Aspirin Conc % w/w	Mean signal (a.u.)	S.D.	CV	Peak min (a.u.)	Peak Max (a.u.)	Noise (a.u.)	S/N
75 g Avicel + 40 g Aspirin	35	4.414478	1.132033	25.64	2.426300	6.866400	4.440100	0.99
75 g Avicel + 30 g Aspirin	29	3.346343	0.875091	26.15	1.828000	5.494600	3.666600	0.91
75 g Avicel + 20 g Aspirin	21	2.672216	0.827909	30.98	1.551300	5.574300	4.023000	0.66
75g Avicel + 10 g Aspirin	12	1.810737	0.461348	25.48	1.062600	2.925900	1.863300	0.97
75 g Avicel + 5 g Aspirin	6	1.618010	0.375656	23.22	1.020700	2.700100	1.679400	0.96
75 g Avicel	0	1.490814	0.418413	28.07	0.729500	2.436200	1.706700	0.87

**Table 37.** AE calibration data calculated from area signals between 10 to 300 kHz, over 200 s from when the AE signal reached a constant value after the addition of different masses of aspirin, particle size 250 - 300 µm, to 75 g Avicel; mixing at impeller speed 50 rpm. AE signals acquired with the WD transducer.

Mixture	Aspirin Conc % w/w	Mean signal (a.u.)	S.D.	CV	Peak min (a.u.)	Peak Max (a.u.)	Noise (a.u.)	S/N
75 g Avicel + 40 g Aspirin	35	8.227788	1.966000	23.89	5.398900	14.920000	9.521100	0.86
75 g Avicel + 30 g Aspirin	29	5.208790	1.155857	22.19	2.767500	8.021400	5.253900	0.99
75 g Avicel + 20 g Aspirin	21	3.565168	0.861978	24.18	2.161600	6.322100	4.160500	0.86
75g Avicel + 10 g Aspirin	12	2.451624	0.553994	22.60	1.557600	4.066200	2.508600	0.98
75 g Avicel + 5 g Aspirin	6	2.015724	0.438057	21.73	1.418300	3.178300	1.760000	1.15
75 g Avicel	0	1.513942	0.344206	22.74	0.931940	2.641200	1.709260	0.89

**Table 38.** AE calibration data calculated from area signals between 10 to 300 kHz, over 200 s from when the AE signal reached a constant value after the addition of different masses of aspirin, particle size 425 – 500 µm, to 75 g Avicel; mixing at impeller speed 50 rpm. AE signals acquired with the WD transducer.

Mixture	Aspirin Conc % w/w	Mean signal (a.u.)	S.D.	CV	Peak min (a.u.)	Peak Max (a.u.)	Noise (a.u.)
75 g Avicel + 40 g Aspirin	35	10.016729	2.870416	28.66	5.382300	18.714000	13.331700
75 g Avicel + 30 g Aspirin	29	5.544060	1.358197	24.50	3.135600	10.480000	7.344400
75 g Avicel + 20 g Aspirin	21	3.309064	0.884573	26.73	2.163900	5.767400	3.603500
75g Avicel + 10 g Aspirin	12	2.253069	0.555245	24.64	1.322000	3.700100	2.378100
75 g Avicel + 5 g Aspirin	6	1.747668	0.359563	20.57	1.134700	2.691500	1.556800
75 g Avicel	0	1.456107	0.318350	21.86	0.944880	2.469800	1.524920

## 15 APPENDIX 4

### 15.1 NIR monitoring of powder blending

First derivative signal processing (Savitsky – Golay, 5 point and second order polynomial) was applied to NIR spectra to correct for baseline offset and makes the regions undergoing change more obvious. The first derivative spectra for different masses of aspirin added to Avicel are illustrated in Figure 193. The first derivative spectra clearly show that an increase in aspirin concentration leads to an increase in the NIR signal at 1116 nm and 1643 nm, the second and first overtones, respectively.

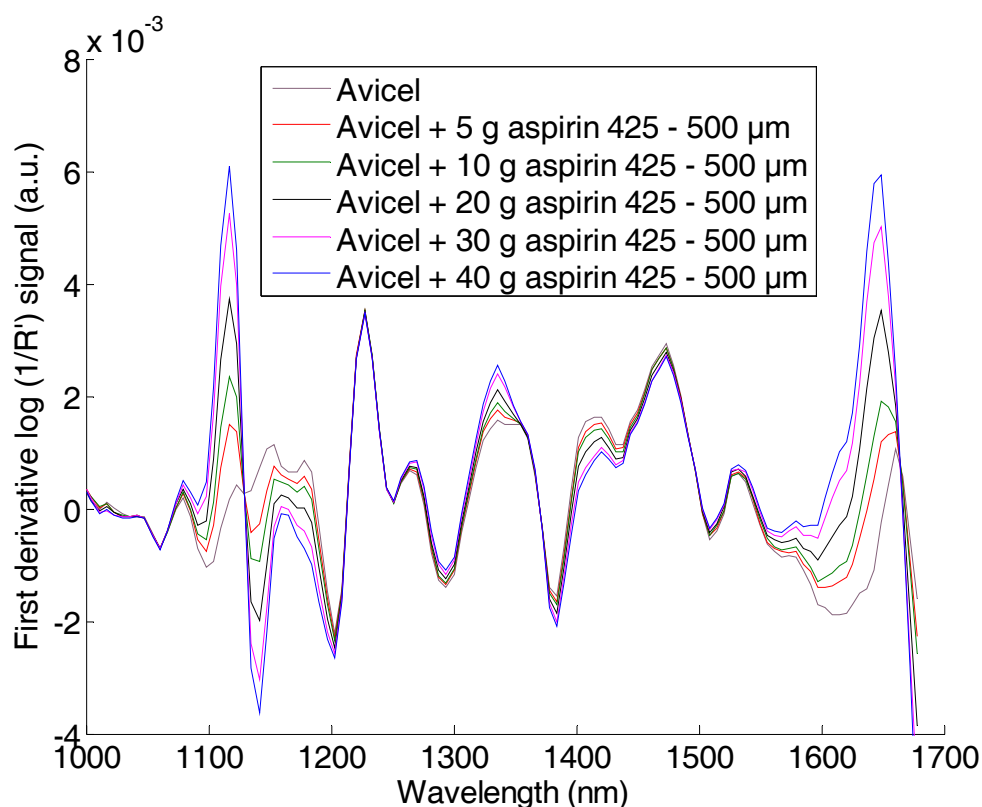


**Figure 193. First derivative log  $1/R'$  NIR spectra at 800 s of increasing masses of aspirin (particle size 425 – 500  $\mu\text{m}$ ) added to Avicel, mixing at impeller speed 50 rpm.**

Mixing profiles were produced for aspirin peaks at 1643.2 nm for each addition of aspirin (see Figure 194). The mixing profile from the first overtone mirrors data obtained in similar experiments in thesis section 12.1.1, and also by Bellamy,<sup>15</sup> where increasing masses of aspirin were added to Avicel PH-101 (un-sieved

therefore constant particle size). A peak in the mixing profile occurs after the addition of aspirin, resulting from the concentration of aspirin moving through the NIR measurement region, before a homogeneous mixture is obtained through further mixing. The magnitude of the signals at steady state increase with increasing mass of aspirin

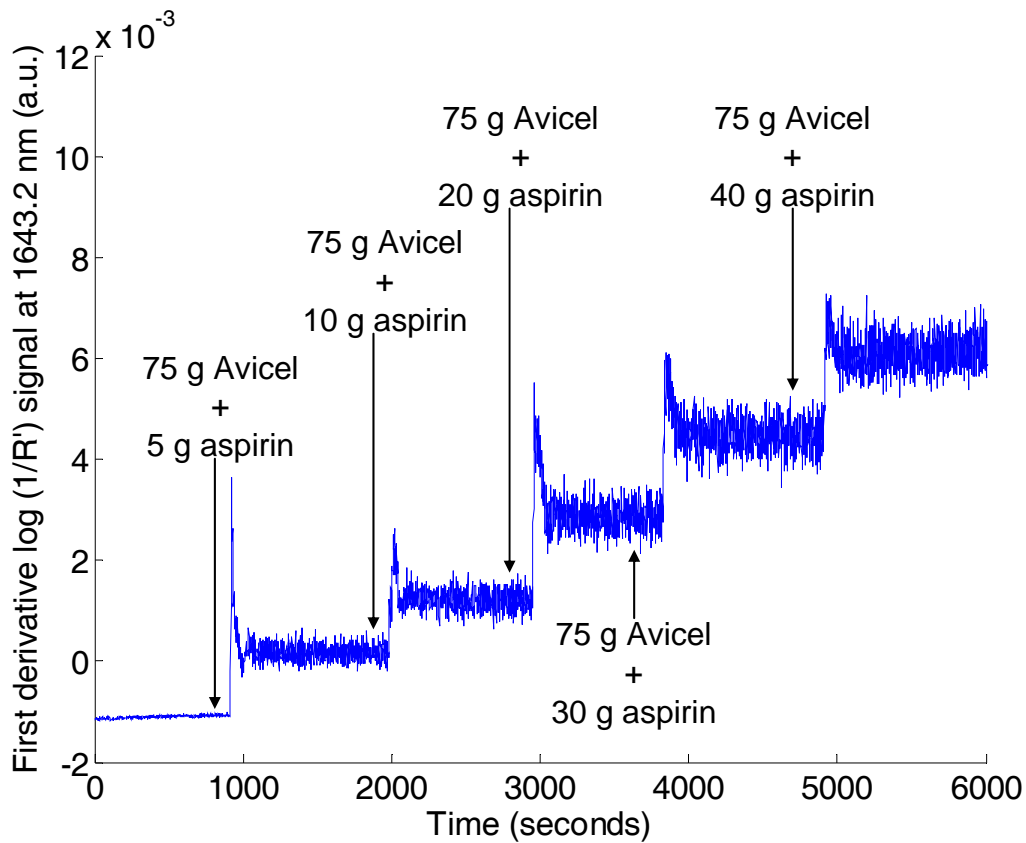


**Figure 194.** NIR mixing profile of first derivative signals at 1643.2 nm, for mixture of increasing masses of aspirin (particle size 425 – 500  $\mu\text{m}$ ) with 75 g Avicel PH-101, mixing at 50 rpm.

The mean signal, standard deviation, CV and peak-to-peak noise have been calculated from the mixing profiles and are illustrated in Table 39 to Table 44.

**Table 39.** NIR calibration data for over 200 s of data calculated from when signals at 1643.2 nm reached a constant value after the addition of aspirin, particle size 425 – 500 µm, to 75 g Avicel, mixing at impeller speed 50 rpm.

Mixture	Aspirin Conc % w/w	Mean signal (a.u.)	S.D.	CV	Peak min (a.u.)	Peak Max (a.u.)	Noise (a.u.)
75 g Avicel + 40 g Aspirin	35	0.006160	0.000274	4.45	0.005560	0.006753	0.001193
75 g Avicel + 30 g Aspirin	29	0.004490	0.000296	6.58	0.003707	0.005114	0.001407
75 g Avicel + 20 g Aspirin	21	0.002872	0.000253	8.82	0.002297	0.003439	0.001142
75g Avicel + 10 g Aspirin	12	0.001201	0.000187	15.57	0.000771	0.001621	0.000850
75 g Avicel + 5 g Aspirin	6	0.000160	0.000135	84.73	-0.000095	0.000471	0.000565
75 g Aspirin	0	-0.001081	0.000017	-1.60	-0.001117	-0.001043	0.000074

**Table 40.** NIR calibration data for over 200 s of data calculated from when signals at 1116.5 nm reached a constant value after the addition of aspirin, particle size 425 – 500 µm, to 75 g Avicel, mixing at impeller speed 50 rpm.

Mixture	Aspirin Conc % w/w	Mean signal (a.u.)	S.D.	CV	Peak min (a.u.)	Peak Max (a.u.)	Noise (a.u.)
75 g Avicel + 40 g Aspirin	35	0.006427	0.000219	3.41	0.005968	0.006900	0.000932
75 g Avicel + 30 g Aspirin	29	0.005068	0.000227	4.49	0.004510	0.005570	0.001060
75 g Avicel + 20 g Aspirin	21	0.003772	0.000178	4.73	0.003405	0.004235	0.000830
75g Avicel + 10 g Aspirin	12	0.002320	0.000129	5.55	0.002025	0.002616	0.000592
75 g Avicel + 5 g Aspirin	6	0.001374	0.000097	7.09	0.001163	0.001611	0.000448
75 g Aspirin	0	0.000167	0.000014	8.23	0.000140	0.000197	0.000057

**Table 41.** NIR calibration data for over 200 s of data calculated from when signals at 1643.2 nm reached a constant value after the addition of aspirin, particle size 250 – 300 µm, to 75 g Avicel, mixing at impeller speed 50 rpm.

Mixture	Aspirin Conc % w/w	Mean signal (a.u.)	S.D.	CV	Peak min (a.u.)	Peak Max (a.u.)	Noise (a.u.)
75 g Avicel + 40 g Aspirin	35	0.011523	0.000281	2.44	0.010908	0.012114	0.001205
75 g Avicel + 30 g Aspirin	29	0.009160	0.000306	3.34	0.008480	0.009857	0.001377
75 g Avicel + 20 g Aspirin	21	0.006458	0.000295	4.57	0.005908	0.007093	0.001185
75g Avicel + 10 g Aspirin	12	0.003007	0.000215	7.15	0.002465	0.003464	0.000999
75 g Avicel + 5 g Aspirin	6	0.001025	0.000169	16.49	0.000617	0.001356	0.000738
75 g Aspirin	0	-0.001185	0.000016	-1.37	-0.001222	-0.001151	0.000071

**Table 42.** NIR calibration data for over 200 s of data calculated from when signals at 1116.5 nm reached a constant value after the addition of aspirin, particle size 250 – 300 µm, to 75 g Avicel, mixing at impeller speed 50 rpm.

Mixture	Aspirin Conc % w/w	Mean signal (a.u.)	S.D.	CV	Peak min (a.u.)	Peak Max (a.u.)	Noise (a.u.)
75 g Avicel + 40 g Aspirin	35	0.007097	0.000131	1.84	0.006812	0.007380	0.000568
75 g Avicel + 30 g Aspirin	29	0.005734	0.000127	2.22	0.005402	0.005995	0.000593
75 g Avicel + 20 g Aspirin	21	0.004260	0.000110	2.58	0.003995	0.004488	0.000493
75g Avicel + 10 g Aspirin	12	0.002415	0.000080	3.31	0.002219	0.002574	0.000354
75 g Avicel + 5 g Aspirin	6	0.001300	0.000061	4.68	0.001160	0.001426	0.000267
75 g Aspirin	0	-0.000042	0.000013	-31.09	-0.000066	-0.000017	0.000049

**Table 43.** NIR calibration data for over 200 s of data calculated from when signals at 1643.2 nm reached a constant value after the addition of aspirin, particle size < 106 µm, to 75 g Avicel, mixing at impeller speed 50 rpm.

Mixture	Aspirin Conc % w/w	Mean signal (a.u.)	S.D.	CV	Peak min (a.u.)	Peak Max (a.u.)	Noise (a.u.)
75 g Avicel + 40 g Aspirin	35	0.016468	0.000195	1.18	0.016040	0.016887	0.000846
75 g Avicel + 30 g Aspirin	29	0.014258	0.000284	1.99	0.013535	0.014852	0.001317
75 g Avicel + 20 g Aspirin	21	0.010834	0.000213	1.97	0.010338	0.011287	0.000949
75g Avicel + 10 g Aspirin	12	0.005811	0.000187	3.21	0.005358	0.006183	0.000825
75 g Avicel + 5 g Aspirin	6	0.002598	0.000107	4.11	0.002357	0.002817	0.000459
75 g Aspirin	0	-0.000832	0.000015	-1.83	-0.000869	-0.000803	0.000066

**Table 44.** NIR calibration data for over 200 s of data calculated from when signals at 1116.5 nm reached a constant value after the addition of aspirin, particle size < 106 µm, to 75 g Avicel, mixing at impeller speed 50 rpm.

Mixture	Aspirin Conc % w/w	Mean signal (a.u.)	S.D.	CV	Peak min (a.u.)	Peak Max (a.u.)	Noise (a.u.)
75 g Avicel + 40 g Aspirin	35	0.006731	0.000070	1.04	0.006585	0.006882	0.000297
75 g Avicel + 30 g Aspirin	29	0.005636	0.000068	1.22	0.005479	0.005788	0.000309
75 g Avicel + 20 g Aspirin	21	0.004323	0.000050	1.17	0.004210	0.004436	0.000226
75g Avicel + 10 g Aspirin	12	0.002556	0.000039	1.53	0.002469	0.002643	0.000174
75 g Avicel + 5 g Aspirin	6	0.001448	0.000022	1.54	0.001401	0.001496	0.000096
75 g Aspirin	0	0.000149	0.000010	6.65	0.000128	0.000175	0.000047

The average intensity over 200 seconds from when a constant signal was reached after the addition of aspirin for the first overtone 1643.2 nm and second overtone 1116.5 nm was plotted (refer to Figure 195 and Figure 196, respectively). The same trends as those observed in thesis section 12.1.1, and by Bellamy<sup>15</sup> were obtained: the average first derivative signal for the first and second overtones increased with increasing mass of aspirin at each particle size, to give an approximately linear response. The first overtone (1643.2 nm) illustrates a decrease in signal intensity at each mass of aspirin with increasing particle size. Deeper information depths occur at second overtone peaks, therefore, a greater volume of sample can be analyzed, which can remove some of the influence from the variation in particle size, through multiple scattering.

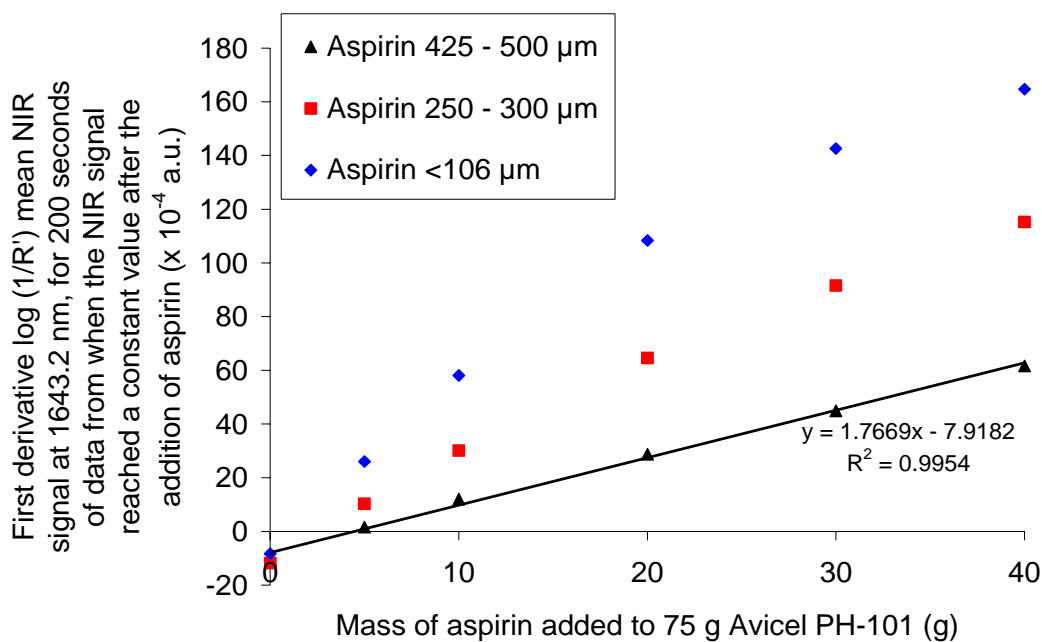


**Figure 195. Average first derivative log (1/R') at 1643.2 nm over 200 seconds of data from when signals reached a constant value after the addition of aspirin, of varying particle size and mass, added to 75 g Avicel PH-101, mixing at 50 rpm.**

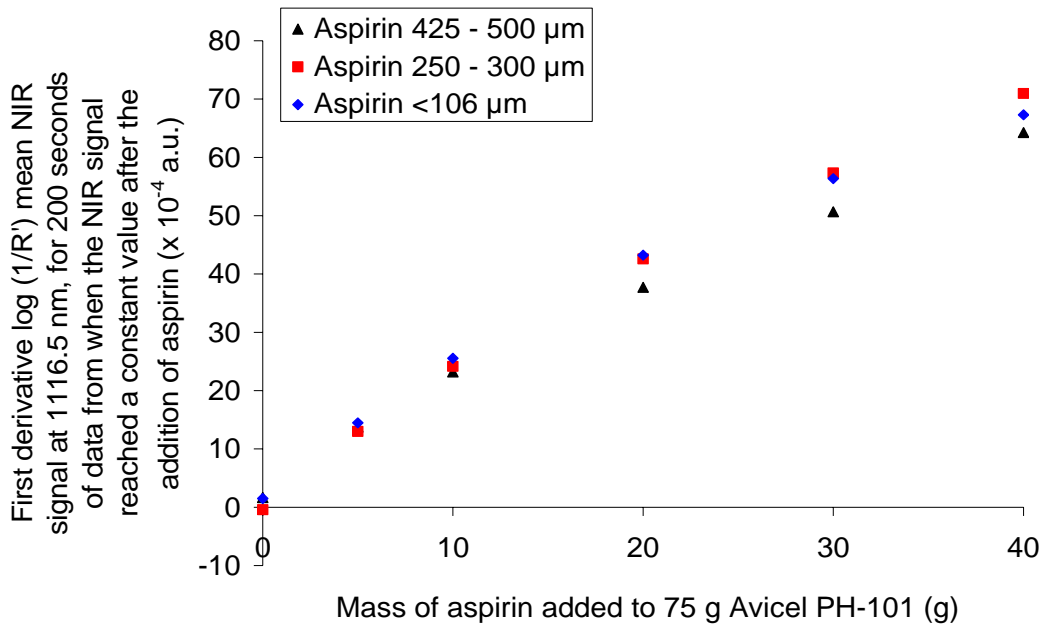


**Figure 196.** Average first derivative log ( $1/R'$ ) at 1116.5 nm over 200 seconds of data from when signals reached a constant value after the addition of aspirin, of varying particle size and mass, added to 75 g Avicel PH-101, mixing at 50 rpm.

The peak-to peak noise of the constant signal in the blending profile for the second overtone peak of aspirin at 1116.5 nm, increased with particle size for each mass of aspirin added to Avicel until a maximum was reached, between 20 and 30 g aspirin added to Avicel (see Figure 197). A similar trend was observed by Bellamy.<sup>15</sup> The variation in signal is caused by the aspirin particles moving into and away from the observation region of the NIR spectrometer, this will be much greater for the larger particle size fractions than for the more abundant smaller particle size fractions.

Only the mixing profiles based on the second overtone aspirin peak displayed the trend of increasing peak-to peak noise with particle size. The first overtone signals showed a similar peak-to-peak noise for the medium and large aspirin particle size ranges (particle size 250 – 300  $\mu\text{m}$  and 425 – 500  $\mu\text{m}$  in comparison to the small aspirin particle size range, < 106  $\mu\text{m}$  (see Figure 198). However, all three aspirin particle size ranges reached a maximum peak-to peak noise between 20 and 40 g aspirin. Deeper information depths occur at second overtone peaks, therefore a greater volume of sample can be analyzed, which can remove some of the influence from the variation in particle size, through multiple scattering.

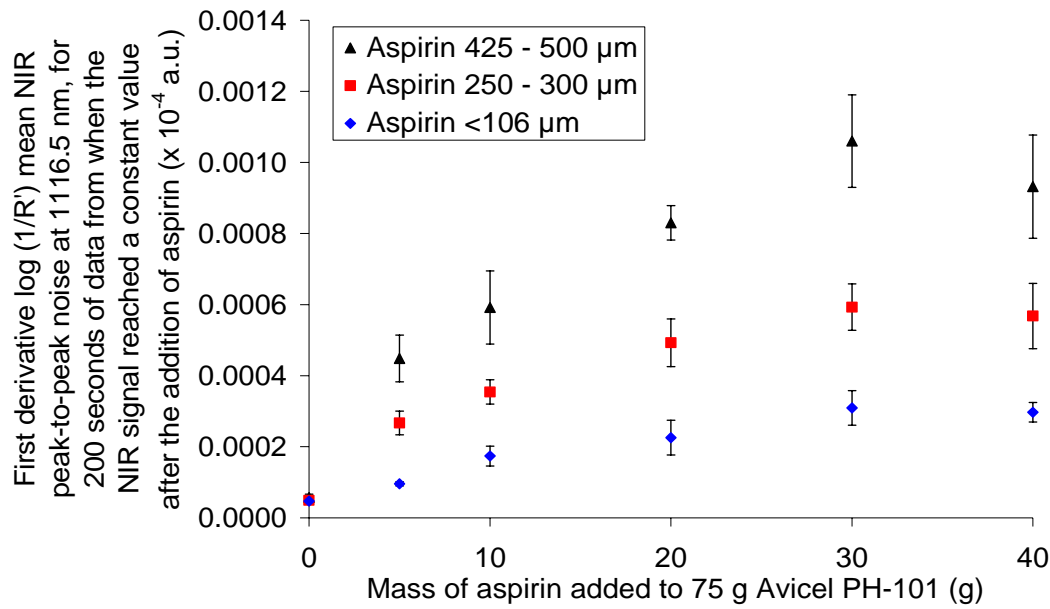


**Figure 197.** NIR peak-to-peak noise of first derivative log (1/R') at 1116.5 nm over 200 seconds of data (in 50 s intervals) from when signals reached a constant value after the addition of aspirin, of varying particle size and mass, added to 75 g Avicel PH-101, mixing at 50 rpm. Each point is the mean of 4 values  $\pm$  one standard deviation.

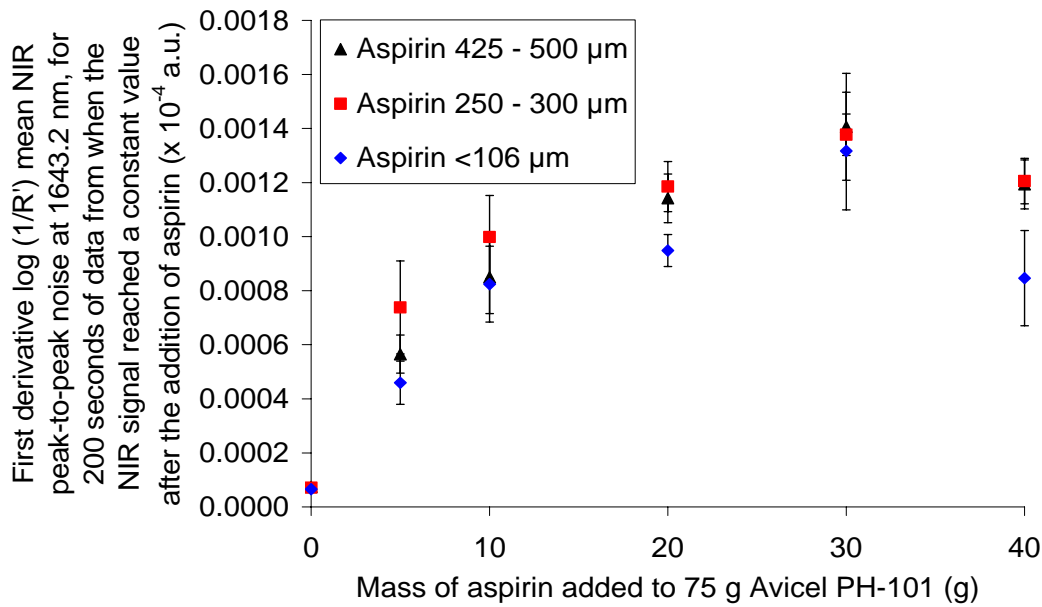


**Figure 198.** Peak-to-peak noise of first derivative log (1/R') at 1643.2 nm over 200 seconds of data (in 50 s intervals) from when signals reached a constant value after the addition of aspirin, of varying particle size and mass, added to 75 g Avicel PH-101, mixing at 50 rpm. Each point is the mean of 4 values  $\pm$  one standard deviation.

## 16 APPENDIX 5

### 16.1 AE monitoring of powder blending at pilot scale

**Table 45.** AE data calculated from area signals between 2 to 460 kHz at timed intervals of 100 seconds throughout the blending of 6 kg of Avicel (small particle size) and 6 kg pot-clav (batch 1), carried out in the ribbon blender at pilot scale with a constant impeller speed.

Time (seconds)	Mean signal (a.u.)	S.D.	CV	Peak min (a.u.)	Peak Max (a.u.)	Peak-to-peak noise (a.u.)
0 - 100	65.1	36.1	55.5	19.0	173.3	154.3
100 - 200	40.9	13.5	32.9	15.2	67.4	52.2
200 - 300	41.2	14.1	34.3	18.8	74.1	55.3
300 - 400	41.6	14.0	33.6	19.0	77.2	58.2
400 - 500	41.7	14.5	34.8	17.5	69.8	52.3
500 - 600	42.4	14.6	34.5	21.2	80.0	58.8
600 - 700	43.4	16.1	37.2	17.3	77.2	59.9
700 - 800	42.4	15.0	35.4	16.1	68.6	52.5
800 - 900	44.3	15.2	34.3	17.1	74.4	57.3
900 - 1000	42.6	15.3	36.0	18.8	75.3	56.5
1000 - 1100	42.1	14.0	33.4	20.5	80.1	59.6
1100 - 1200	42.4	15.1	35.6	17.1	79.4	62.2
1200 - 1300	43.7	15.1	34.5	18.5	71.5	53.0
1300 - 1400	43.3	14.7	34.0	19.3	81.4	62.1
1400 - 1500	41.9	15.7	37.4	16.5	80.2	63.7
1500 - 1600	43.4	15.0	34.6	19.6	71.2	51.5
1600 - 1700	42.4	14.8	34.8	20.1	71.2	51.1
1700 - 1800	41.8	13.8	33.0	19.2	64.7	45.5

**Table 46.** AE data calculated from area signals between 2 to 460 kHz at timed intervals of 100 seconds throughout the blending of 6 kg of Avicel (small particle size) and 6 kg pot-clav (batch 2), carried out in the ribbon blender at pilot scale with a constant impeller speed.

Time (seconds)	Mean signal (a.u.)	S.D.	CV	Peak min (a.u.)	Peak Max (a.u.)	Peak-to-peak noise (a.u.)
0 - 100	82.1	46.6	56.8	24.7	244.1	219.4
100 - 200	43.1	18.0	41.8	15.7	79.4	63.8
200 - 300	39.1	14.4	36.9	14.9	69.1	54.2
300 - 400	38.8	15.4	39.8	15.8	61.8	46.0
400 - 500	38.9	14.6	37.6	15.1	68.1	53.0
500 - 600	40.0	15.8	39.5	16.1	69.3	53.2
600 - 700	39.6	15.5	39.2	16.1	67.0	50.9
700 - 800	39.6	16.4	41.3	16.8	77.1	60.3
800 - 900	40.0	16.2	40.4	15.6	71.0	55.4
900 - 1000	39.1	16.0	40.8	14.8	63.4	48.6
1000 - 1100	38.6	14.8	38.5	16.0	67.1	51.1
1100 - 1200	38.3	15.0	39.1	16.4	68.3	51.9
1200 - 1300	38.2	15.8	41.5	15.9	73.1	57.2
1300 - 1400	39.0	16.4	42.1	16.0	70.2	54.2
1400 - 1500	38.9	14.8	38.2	15.2	69.0	53.8
1500 - 1600	37.9	14.5	38.2	13.9	68.0	54.2
1600 - 1700	39.1	15.2	39.0	18.3	68.0	49.8
1700 - 1800	37.5	15.1	40.4	13.6	66.2	52.5

**Table 47.** AE data calculated from area signals between 2 to 460 kHz at timed intervals of 100 seconds throughout the blending of 5 kg of Avicel (small particle size) and 5 kg pot-clav (batch 3), carried out in the ribbon blender at pilot scale with a constant impeller speed.

Time (seconds)	Mean signal (a.u.)	S.D.	CV	Peak min (a.u.)	Peak Max (a.u.)	Peak-to-peak noise (a.u.)
0 - 100	96.2	49.6	51.6	26.7	212.4	185.7
100 - 200	66.1	30.2	45.7	22.7	134.7	112.1
200 - 300	60.8	25.6	42.0	20.4	106.2	85.8
300 - 400	62.3	29.1	46.6	19.7	119.0	99.3
400 - 500	60.9	24.2	39.7	20.9	110.2	89.4
500 - 600	60.6	27.4	45.1	24.7	111.2	86.5
600 - 700	62.6	28.4	45.4	21.5	108.1	86.6
700 - 800	61.0	28.2	46.2	21.5	112.0	90.5
800 - 900	62.6	28.3	45.2	24.3	125.2	100.9
900 - 1000	59.5	28.0	47.1	21.4	109.9	88.5
1000 - 1100	61.6	27.7	45.0	22.8	117.0	94.2
1100 - 1200	61.7	26.8	43.5	23.0	120.1	97.1
1200 - 1300	62.5	30.1	48.1	23.3	128.2	104.9
1300 - 1400	61.7	28.3	45.8	22.3	119.5	97.2
1400 - 1500	59.6	27.1	45.4	22.0	106.5	84.5
1500 - 1600	59.2	25.9	43.8	22.1	105.2	83.1
1600 - 1700	60.4	27.4	45.4	23.9	105.2	81.3
1700 - 1800	58.5	27.3	46.6	19.4	121.2	101.8

**Table 48.** AE data calculated from area signals between 2 to 460 kHz at timed intervals of 100 seconds throughout the blending of 5 kg of Avicel (large particle size) and 5 kg pot-clav (batch 4), carried out in the ribbon blender at pilot scale with a constant impeller speed.

Time (seconds)	Mean signal (a.u.)	S.D.	CV	Peak min (a.u.)	Peak Max (a.u.)	Peak-to-peak noise (a.u.)
0 - 100	140.3	93.0	66.3	38.6	543.1	504.6
100 - 200	94.1	45.7	48.5	29.2	199.1	169.9
200 - 300	89.4	43.4	48.6	26.3	175.9	149.6
300 - 400	85.8	37.6	43.8	31.4	162.1	130.8
400 - 500	87.8	40.6	46.3	26.1	180.0	153.9
500 - 600	88.8	41.1	46.3	30.5	177.8	147.3
600 - 700	87.3	41.4	47.4	36.3	175.3	139.0
700 - 800	85.0	39.4	46.4	31.2	166.5	135.3
800 - 900	88.2	39.5	44.7	31.5	162.9	131.4
900 - 1000	84.2	40.1	47.6	32.5	162.2	129.8
1000 - 1100	84.3	41.6	49.3	30.0	150.0	120.0
1100 - 1200	83.8	36.3	43.4	30.9	150.8	119.9
1200 - 1300	86.6	38.6	44.6	34.6	177.5	142.9
1300 - 1400	84.4	37.8	44.9	34.9	152.0	117.1
1400 - 1500	85.9	41.4	48.2	32.9	178.4	145.5
1500 - 1600	85.2	41.5	48.7	29.0	169.0	140.0
1600 - 1700	86.2	40.5	47.0	30.5	169.0	138.4
1700 - 1800	84.9	37.8	44.6	38.2	161.5	123.3

**Table 49.** AE data calculated from area signals between 2 to 460 kHz at timed intervals of 100 seconds throughout the blending of 4 kg of Avicel (large particle size) and 4 kg pot-clav (batch 1), carried out in the ribbon blender at pilot scale with a constant impeller speed.

Time (seconds)	Mean signal (a.u.)	S.D.	CV	Peak min (a.u.)	Peak Max (a.u.)	Peak-to-peak noise (a.u.)
0 - 100	37.1	33.0	89.0	8.3	219.8	211.5
100 - 200	19.5	10.0	51.6	5.3	41.5	36.2
200 - 300	17.2	8.8	51.5	5.1	34.7	29.6
300 - 400	18.3	8.9	48.7	5.3	33.9	28.5
400 - 500	18.4	8.7	47.1	6.5	34.2	27.7
500 - 600	17.3	8.1	46.8	5.9	34.7	28.8
600 - 700	17.8	8.5	47.8	5.5	33.6	28.1
700 - 800	18.1	8.6	47.2	5.5	32.9	27.4
800 - 900	18.0	8.7	48.5	5.3	34.8	29.5
900 - 1000	17.1	8.2	48.1	5.9	34.7	28.8
1000 - 1100	18.1	8.7	47.8	4.5	36.2	31.7
1100 - 1200	18.2	8.8	48.3	5.4	34.7	29.2
1200 - 1300	17.6	8.3	46.8	4.8	35.0	30.2
1300 - 1400	16.9	8.0	47.5	5.0	31.7	26.7
1400 - 1500	17.1	7.7	45.2	5.2	31.7	26.5
1500 - 1600	17.1	8.2	48.2	5.9	31.7	25.8
1600 - 1700	16.8	8.3	49.3	4.9	34.1	29.1
1700 - 1800	17.5	8.1	46.6	5.7	33.7	28.0

**Table 50.** AE data calculated from area signals between 2 to 460 kHz at timed intervals of 100 seconds throughout the blending of 4 kg of Avicel (large particle size) and 4 kg pot-clav (batch 2), carried out in the ribbon blender at pilot-scale with a constant impeller speed.

Time (seconds)	Mean signal (a.u.)	S.D.	CV	Peak min (a.u.)	Peak Max (a.u.)	Peak-to-peak noise (a.u.)
0 - 100	76.9	55.9	72.6	18.9	371.2	352.2
100 - 200	43.0	20.3	47.1	10.5	84.0	73.5
200 - 300	39.6	17.5	44.2	11.0	67.5	56.5
300 - 400	38.3	16.6	43.4	12.2	73.5	61.3
400 - 500	37.5	16.4	43.6	12.7	65.5	52.7
500 - 600	36.0	15.6	43.3	11.7	61.5	49.8
600 - 700	36.0	15.8	43.8	12.1	62.6	50.5
700 - 800	34.6	14.7	42.4	12.2	62.0	49.8
800 - 900	34.5	15.9	46.0	12.2	61.7	49.5
900 - 1000	34.1	15.8	46.3	11.8	59.2	47.4
1000 - 1100	34.3	15.6	45.6	10.6	62.4	51.7
1100 - 1200	34.2	15.5	45.2	12.0	65.9	53.9
1200 - 1300	33.4	14.0	41.8	11.1	58.0	47.0
1300 - 1400	34.1	14.9	43.7	12.0	60.2	48.2
1400 - 1500	34.1	14.8	43.5	12.2	58.5	46.3
1500 - 1600	34.2	15.3	44.6	10.4	64.4	54.0
1600 - 1700	33.6	15.5	46.2	11.7	64.4	52.7
1700 - 1800	34.6	15.7	45.5	11.0	73.0	62.0

## 17 APPENDIX 6

### 17.1 Preliminary investigation of butanol feed rate

**Table 51.** Mean butanol feed rate acquired for five repeat standard esterification reactions, carried out at 40 °C in the 10 L CoFlux® reactor.

Mean time (s)	SD - time (s)	CV - time (%)	Mean butanol feed (g)	SD - butanol feed (g)	CV - butanol feed (%)
0	0	0	0	0	0
20	0	0	43.22	6	15
40	0	0	119.68	8	7
60	0	0	197.96	9	5
80	0	0	274.22	8	3
100	0	0	350.18	9	3
120	0	0	426.22	11	3
141	0	0	503.62	13	3
161	0	0	579.42	16	3
181	0	0	656	17	3
201	0	0	732.92	19	3
221	0	0	808	23	3
241	0	0	884.54	25	3
261	0	0	957.54	22	2
281	0	0	1034.46	26	2
301	0	0	1105.78	30	3
321	0	0	1184.56	29	2
341	0	0	1252.2	33	3
361	0	0	1329.54	37	3
381	0	0	1406.1	33	2
401	0	0	1479.6	36	2
422	0	0	1552.82	38	2
442	0	0	1628.64	40	2
462	0	0	1693.56	34	2
482	0	0	1775.66	44	2
502	0	0	1848.34	44	2
522	0	0	1920.92	48	2
542	0	0	1994.66	50	3
562	0	0	2065.44	52	3
582	0	0	2138.6	54	3
602	0	0	2211.52	56	3
622	0	0	2284.46	58	3
642	0	0	2357.3	60	3
662	0	0	2430.26	62	3
682	0	0	2494	55	2
703	0	0	2571.26	67	3
723	0	0	2643.78	69	3
743	0	0	2714.54	69	3
763	0	0	2785.56	73	3
783	0	0	2853.36	78	3
803	0	0	2929.42	78	3
823	0	0	3001.62	80	3
843	0	0	3073.28	82	3
863	0	0	3140.48	85	3
883	0	0	3211.82	87	3
903	0	0	3281.84	87	3
923	0	0	3353.42	89	3
943	0	0	3418.78	89	3
963	0	0	3494.22	96	3
984	0	0	3565.32	98	3
1004	0	0	3636.5	100	3
1024	0	0	3672.175	81	2
1044	0	0	3701.733333	37	1
1064	0	0	3751.2	24	1
1084	0	0	3802.7	0	0

**Table 52.** Mean butanol feed rate acquired for esterification reactions at 30, 50 °C, and five repeat standard reactions, at 40 °C in the 10 L CoFlux® reactor.

Mean time (s)	SD - time (s)	CV - time (%)	Mean butanol feed (g)	SD - butanol feed (g)	CV - butanol feed (%)
0	0	0	0	0	0
20	0	0	42	5	13
40	0	0	120	7	6
60	0	0	198	8	4
80	0	0	275	7	2
100	0	0	352	8	2
120	0	0	429	11	3
141	0	0	506	12	2
161	0	0	583	15	3
181	0	0	661	16	2
201	0	0	738	18	2
221	0	0	815	22	3
241	0	0	891	23	3
261	0	0	965	22	2
281	0	0	1043	25	2
301	0	0	1116	30	3
321	0	0	1194	29	2
341	0	0	1261	31	2
361	0	0	1342	37	3
381	0	0	1419	35	2
401	0	0	1494	38	3
422	0	0	1567	40	3
442	0	0	1644	42	3
462	0	0	1712	43	3
482	0	0	1793	47	3
502	0	0	1868	49	3
522	0	0	1940	51	3
542	0	0	2015	54	3
562	0	0	2087	57	3
582	0	0	2161	59	3
602	0	0	2234	60	3
622	0	0	2309	63	3
642	0	0	2383	66	3
662	0	0	2457	68	3
682	0	0	2522	66	3
703	0	0	2599	73	3
723	0	0	2672	75	3
743	0	0	2744	76	3
763	0	0	2817	80	3
783	0	0	2887	85	3
803	0	0	2963	86	3
823	0	0	3036	88	3
843	0	0	3107	89	3
863	0	0	3176	92	3
883	0	0	3248	95	3
903	0	0	3319	96	3
923	0	0	3392	98	3
943	0	0	3460	102	3
963	0	0	3535	105	3
984	0	0	3607	108	3
1004	0	0	3678	109	3
1024	0	0	3672	81	2
1044	0	0	3702	37	1
1064	0	0	3751	24	1
1084	0	0	3803	0	0

**Table 53. Mean butanol feed rate acquired for esterification reactions with a temperature fault, a water fault and five repeat standard reactions at 40 °C in the 10 L CoFlux® reactor.**

Mean time (s)	SD - time (s)	CV - time (%)	Mean butanol feed (g)	SD - butanol feed (g)	CV - butanol feed (%)
0	0	0	0	0	0
20	0	0	53	14	26
40	0	0	130	17	13
60	0	0	204	11	5
80	0	0	279	8	3
100	0	0	356	11	3
120	0	0	435	15	3
141	0	0	511	15	3
161	0	0	585	15	3
181	0	0	658	13	2
201	0	0	735	16	2
221	0	0	810	18	2
241	0	0	888	19	2
261	0	0	961	18	2
281	0	0	1036	20	2
301	0	0	1108	23	2
321	0	0	1185	22	2
341	0	0	1256	26	2
361	0	0	1332	28	2
381	0	0	1408	25	2
401	0	0	1480	27	2
422	0	0	1553	29	2
442	0	0	1629	30	2
462	0	0	1699	27	2
482	0	0	1781	34	2
502	0	0	1855	35	2
522	0	0	1927	37	2
542	0	0	1999	38	2
562	0	0	2070	40	2
582	0	0	2144	41	2
602	0	0	2218	43	2
622	0	0	2292	45	2
642	0	0	2367	47	2
662	0	0	2440	49	2
682	0	0	2508	46	2
703	0	0	2584	54	2
723	0	0	2657	56	2
743	0	0	2730	56	2
763	0	0	2801	59	2
783	0	0	2871	63	2
803	0	0	2946	63	2
823	0	0	3019	66	2
843	0	0	3095	69	2
863	0	0	3164	72	2
883	0	0	3237	74	2
903	0	0	3308	75	2
923	0	0	3380	76	2
943	0	0	3448	79	2
963	0	0	3524	83	2
983	0	0	3595	85	2
1004	0	0	3668	87	2
1024	0	0	3725	87	2
1044	0	0	3702	37	1
1064	0	0	3751	24	1
1084	0	0	3803	-	0

**Table 54. Mean butanol feed rate acquired for esterification reactions with a 50 % reduction in TMG, a TMG fault and five repeat standard reactions at 40 °C in the 10 L CoFlux® reactor.**

Mean time (s)	SD - time (s)	CV - time (%)	Mean butanol feed (g)	SD - butanol feed (g)	CV - butanol feed (%)
0	0	0	0	0	0
20	0	0	43.22	6	15
40	0	0	119.68	8	7
60	0	0	197.96	9	5
80	0	0	274.22	8	3
100	0	0	350.18	9	3
120	0	0	426.22	11	3
141	0	0	503.62	13	3
161	0	0	579.42	16	3
181	0	0	656	17	3
201	0	0	732.92	19	3
221	0	0	808	23	3
241	0	0	884.54	25	3
261	0	0	957.54	22	2
281	0	0	1034.46	26	2
301	0	0	1105.78	30	3
321	0	0	1184.56	29	2
341	0	0	1252.2	33	3
361	0	0	1329.54	37	3
381	0	0	1406.1	33	2
401	0	0	1479.6	36	2
422	0	0	1552.82	38	2
442	0	0	1628.64	40	2
462	0	0	1693.56	34	2
482	0	0	1775.66	44	2
502	0	0	1848.34	44	2
522	0	0	1920.92	48	2
542	0	0	1994.66	50	3
562	0	0	2065.44	52	3
582	0	0	2138.6	54	3
602	0	0	2211.52	56	3
622	0	0	2284.46	58	3
642	0	0	2357.3	60	3
662	0	0	2430.26	62	3
682	0	0	2494	55	2
703	0	0	2571.26	67	3
723	0	0	2643.78	69	3
743	0	0	2714.54	69	3
763	0	0	2785.56	73	3
783	0	0	2853.36	78	3
803	0	0	2929.42	78	3
823	0	0	3001.62	80	3
843	0	0	3073.28	82	3
863	0	0	3140.48	85	3
883	0	0	3211.82	87	3
903	0	0	3281.84	87	3
923	0	0	3353.42	89	3
943	0	0	3418.78	89	3
963	0	0	3494.22	96	3
984	0	0	3565.32	98	3
1004	0	0	3636.5	100	3
1024	0	0	3672.175	81	2
1044	0	0	3701.733333	37	1
1064	0	0	3751.2	24	1
1084	0	0	3802.7	0	0

## **17.2 Investigation of reactor temperature control**

**Table 55.** Mean temperature data acquired for five repeat standard esterification reactions of butanol with acetic anhydride at 40 °C, carried out in the 10 L CoFlux®reactor. Butanol addition started at zero seconds.

<b>Time (seconds)</b>	<b>Mean standard reaction temperature (°C)</b>	<b>S.D. (°C)</b>	<b>CV (%)</b>
-300	41.57	1	3
0	39.46	0	1
300	40.40	1	1
600	40.50	0	0
900	40.48	0	0
1200	41.06	0	0
1500	40.73	0	0
1800	40.58	0	0
2400	40.47	0	0
3000	40.36	0	0
3600	40.29	0	0
4500	40.20	0	0
5400	40.18	0	0
6300	40.16	0	0
7200	40.10	0	0
9000	40.03	0	0
10800	39.98	0	0

### 17.3 Comparison of enthalpy and GC data

**Table 56.** Mean in-line enthalpy data acquired for five repeat standard esterification reactions of butanol with acetic anhydride at 40 °C, carried out in the 10 L CoFlux® reactor. Butanol addition started at zero seconds.

Time (seconds)	Mean standard reaction enthalpy (kJ)	S.D. (kJ)	CV (%)
-300	145.95	10	7
0	140.04	10	7
300	183.07	29	16
600	276.03	12	4
900	352.39	9	3
1200	476.57	18	4
1500	590.83	14	2
1800	691.43	13	2
2400	847.39	12	1
3000	969.83	13	1
3600	1075.18	11	1
4500	1204.27	12	1
5400	1308.91	15	1
6300	1397.88	17	1
7200	1474.48	19	1
9000	1604.47	28	2
10800	1704.62	30	2

**Table 57.** Mean butyl acetate data acquired from off-line GC analysis for five repeat standard esterification reactions of butanol with acetic anhydride at 40 °C, carried out in the 10 L CoFlux® reactor. Butanol addition started at zero seconds.

Time (seconds)	Mean butyl acetate concentration (moles dm-3)	S.D. (moles dm-3)	CV (%)
-300	0.0	0	0
0	0.0	0	0
300	0.4	0	12
600	0.8	0	5
900	1.0	0	4
1200	1.2	0	6
1500	1.4	0	2
1800	1.6	0	2
2400	1.8	0	4
3000	2.0	0	2
3600	2.2	0	2
4500	2.4	0	3
5400	2.7	0	2
6300	2.8	0	2
7200	2.9	0	2
9000	3.2	0	3
10800	3.3	0	2

#### 17.4 PC1 and PC2 scores from NIR PCA models

**Table 58.** Mean PC1 scores from NIR data acquired for five repeat standard esterification reactions of butanol with acetic anhydride at 40 °C, carried out in the 10 L CoFlux® reactor. Butanol addition started at zero seconds.

Time (seconds)	Mean scores of PC1	S.D.	CV (%)
-300	0.0881	0.0043	5
0	0.0862	0.0009	1
300	0.0524	0.0013	3
600	0.0310	0.0011	4
900	0.0173	0.0010	6
1200	0.0107	0.0005	5
1500	0.0081	0.0005	6
1800	0.0060	0.0005	8
2400	0.0025	0.0005	19
3000	-0.0002	0.0005	297
3600	-0.0024	0.0005	20
4500	-0.0052	0.0005	10
5400	-0.0075	0.0005	7
6300	-0.0094	0.0005	5
7200	-0.0110	0.0005	4
9000	-0.0138	0.0005	4
10800	-0.0160	0.0005	3

**Table 59.** Mean PC2 scores from NIR data acquired for five repeat standard esterification reactions of butanol with acetic anhydride at 40 °C, carried out in the 10 L CoFlux® reactor. Butanol addition started at zero seconds.

Time (seconds)	Mean scores of PC2	S.D.	CV (%)
-300	0.0241	0.0011	5
0	0.0242	0.0005	2
300	0.0003	0.0004	136
600	-0.0118	0.0006	5
900	-0.0198	0.0007	3
1200	-0.0210	0.0003	1
1500	-0.0181	0.0003	1
1800	-0.0157	0.0003	2
2400	-0.0117	0.0002	2
3000	-0.0084	0.0002	3
3600	-0.0057	0.0002	4
4500	-0.0023	0.0003	11
5400	0.0005	0.0003	48
6300	0.0029	0.0003	9
7200	0.0051	0.0002	5
9000	0.0085	0.0002	3
10800	0.0113	0.0003	2

## 17.5 PC1 and PC2 scores from MIR PCA models

**Table 60.** Mean PC1 scores from MIR data acquired for four repeat standard esterification reactions of butanol with acetic anhydride at 40 °C, carried out in the 10 L CoFlux® reactor. Butanol addition started at zero seconds.

Time (seconds)	Mean scores of PC1	S.D.	CV (%)
-300	0.2729	0.0558	20
0	0.2979	0.0119	4
300	0.2154	0.0077	4
600	0.1470	0.0065	4
900	0.1006	0.0067	7
1200	0.0782	0.0041	5
1500	0.0600	0.0067	11
1800	0.0480	0.0024	5
2400	0.0276	0.0037	13
3000	0.0100	0.0029	29
3600	0.0011	0.0060	569
4500	-0.0133	0.0056	42
5400	-0.0326	0.0049	15
6300	-0.0445	0.0063	14
7200	-0.0531	0.0043	8
9000	-0.0717	0.0074	10
10800	-0.0857	0.0059	7

**Table 61.** Mean PC2 scores from MIR data acquired for five repeat standard esterification reactions of butanol with acetic anhydride at 40 °C, carried out in the 10 L CoFlux® reactor. Butanol addition started at zero secondsPC2.

Time (seconds)	Mean scores of PC2	S.D.	CV (%)
-300	0.0463	0.0241	52
0	0.0535	0.0048	9
300	0.0077	0.0059	76
600	-0.0216	0.0024	11
900	-0.0334	0.0018	5
1200	-0.0352	0.0026	7
1500	-0.0301	0.0012	4
1800	-0.0271	0.0024	9
2400	-0.0228	0.0013	6
3000	-0.0169	0.0014	8
3600	-0.0111	0.0026	23
4500	-0.0033	0.0042	128
5400	-0.0024	0.0032	135
6300	0.0030	0.0032	106
7200	0.0060	0.0014	23
9000	0.0124	0.0021	17
10800	0.0200	0.0016	8

## 17.6 Prediction of butyl acetate concentrations from NIR PLS models

**Table 62.** Percentage error of measured and predicted (using NIR PLS model number 1, in section 8.2.4, Table 11) concentrations of butyl acetate for standard reaction number 1 at 40 °C (see thesis section 8.2.2, Table 8), carried out in the 10 L CoFlux® reactor. Butanol addition started at zero seconds.

Time (seconds)	Butyl acetate concentration (moles dm-3) for standard reaction 1, at 40 °C		Error as a % of butyl acetate concentration
	Measured	PLS model number 1 prediction	
-300	0.00	0.03	-
0	0.00	0.02	-
300	0.49	0.51	5
600	0.75	0.85	13
900	0.97	1.03	6
1200	1.14	1.22	8
1500	1.36	1.42	5
1800	1.53	1.59	4
2400	1.76	1.87	6
3000	1.97	2.09	6
3600	2.16	2.27	5
4500	2.34	2.50	7
5400	2.61	2.70	3
6300	2.71	2.86	6
7200	2.86	3.00	5
9000	3.07	3.24	6
10800	3.21	3.43	7

**Table 63.** Percentage error of measured and predicted (using NIR PLS model number 2, in section 8.2.4, Table 11) concentrations of butyl acetate for standard reaction number 2 at 40 °C (see thesis section 8.2.2, Table 8), carried out in the 10 L CoFlux® reactor. Butanol addition started at zero seconds.

Time (seconds)	Butyl acetate concentration (moles dm-3) for standard reaction 2, at 40 °C		Error as a % of butyl acetate concentration
	Measured	PLS model number 2 prediction	
-300	0.00	0.04	-
0	0.00	0.06	-
300	0.43	0.57	32
600	0.75	0.87	15
900	0.95	1.02	8
1200	1.14	1.19	4
1500	1.34	1.39	4
1800	1.54	1.55	1
2400	1.79	1.82	2
3000	2.03	2.04	1
3600	2.21	2.22	1
4500	2.48	2.46	-1
5400	2.65	2.65	0
6300	2.80	2.81	0
7200	3.02	2.95	-2
9000	3.21	3.18	-1
10800	3.36	3.37	0

**Table 64.** Percentage error of measured and predicted (using NIR PLS model number 3, in section 8.2.4, Table 11) concentrations of butyl acetate for standard reaction number 3 at 40 °C (see thesis section 8.2.2, Table 8), carried out in the 10 L CoFlux® reactor. Butanol addition started at zero seconds.

Time (seconds)	Butyl acetate concentration (moles dm-3) for standard reaction 3, at 40 °C		Error as a % of butyl acetate concentration
	Measured	PLS model number 3 prediction	
-300	0.00	0.45	-
0	0.00	-0.04	-
300	0.40	0.40	1
600	0.74	0.76	3
900	0.97	0.96	-1
1200	1.13	1.15	1
1500	1.38	1.35	-2
1800	1.56	1.52	-2
2400	1.81	1.80	-1
3000	2.06	2.02	-2
3600	2.27	2.20	-3
4500	2.43	2.43	0
5400	2.70	2.62	-3
6300	2.77	2.79	0
7200	2.86	2.93	2
9000	3.16	3.16	0
10800	3.39	3.35	-1

**Table 65.** Percentage error of measured and predicted (using NIR PLS model number 4, in section 8.2.4, Table 11) concentrations of butyl acetate for standard reaction number 4 at 40 °C (see thesis section 8.2.2, Table 8), carried out in the 10 L CoFlux® reactor. Butanol addition started at zero seconds.

Time (seconds)	Butyl acetate concentration (moles dm-3) for standard reaction 4, at 40 °C		Error as a % of butyl acetate concentration
	Measured	PLS model number 4 prediction	
-300	0.00	0.04	-
0	0.00	0.01	-
300	0.38	0.52	39
600	0.80	0.83	4
900	0.97	0.98	1
1200	1.25	1.18	-6
1500	1.40	1.38	-1
1800	1.54	1.55	0
2400	1.88	1.82	-3
3000	2.06	2.04	-1
3600	2.22	2.22	0
4500	2.50	2.45	-2
5400	2.65	2.64	0
6300	2.84	2.81	-1
7200	2.96	2.95	0
9000	3.20	3.19	0
10800	3.33	3.38	2

**Table 66.** Percentage error of measured and predicted (using NIR PLS model number 5, in section 8.2.4, Table 11) concentrations of butyl acetate for standard reaction number 5 at 40 °C (see thesis section 8.2.2, Table 8), carried out in the 10 L CoFlux® reactor. Butanol addition started at zero seconds.

Time (seconds)	Butyl acetate concentration (moles dm-3) for standard reaction 5, at 40 °C		Error as a % of butyl acetate concentration
	Measured	PLS model number 5 prediction	
-300	0.00	-0.02	-
0	0.00	-0.02	-
300	0.49	0.45	-9
600	0.83	0.78	-5
900	1.06	0.95	-10
1200	1.26	1.14	-9
1500	1.39	1.34	-3
1800	1.60	1.51	-6
2400	1.96	1.79	-9
3000	2.11	2.01	-5
3600	2.25	2.19	-3
4500	2.42	2.42	0
5400	2.72	2.61	-4
6300	2.89	2.78	-4
7200	2.97	2.92	-2
9000	3.34	3.16	-5
10800	3.37	3.35	-1

**Table 67.** Percentage error of measured and predicted (using NIR PLS model number 6, in section 8.2.4, Table 11) concentrations of butyl acetate for standard reaction number 6 at 40 °C with an increased butanol feed rate (see thesis section 8.2.2, Table 8), carried out in the 10 L CoFlux® reactor. Butanol addition started at zero seconds.

Time (seconds)	Butyl acetate concentration (moles dm-3) for reaction 6, with an increased butanol feed rate		Error as a % of butyl acetate concentration
	Measured	PLS model number 6 prediction	
-300	0.00	-0.02	-
0	0.00	0.03	-
300	-	0.53	-
600	0.85	0.81	-5
900	1.19	1.11	-7
1200	1.44	1.33	-8
1500	1.72	1.51	-12
1800	1.74	1.66	-4
2400	2.09	1.92	-8
3000	2.16	2.13	-2
3600	2.27	2.30	1
4500	2.50	2.51	1
5400	2.63	2.69	2
6300	2.85	2.85	0
7200	2.85	2.98	5
9000	3.14	3.21	2
10800	3.26	3.39	4

**Table 68.** Percentage error of measured and predicted (using NIR PLS model number 7, in section 8.2.4, Table 11) concentrations of butyl acetate for standard reaction number 7 at 30 °C (see thesis section 8.2.2, Table 8), carried out in the 10 L CoFlux® reactor. Butanol addition started at zero seconds.

Time (seconds)	Butyl acetate concentration (moles dm-3) for reaction 7, at 30 °C		Error as a % of butyl acetate concentration
	Measured	PLS model number 7 prediction	
-300	0.00	-0.18	-
0	0.00	-0.16	-
300	0.31	0.32	4
600	0.56	0.49	-11
900	0.74	0.64	-13
1200	0.87	0.81	-7
1500	1.06	0.96	-9
1800	1.16	1.09	-6
2400	1.34	1.30	-3
3000	1.51	1.48	-2
3600	1.76	1.65	-7
4500	1.88	1.84	-2
5400	2.05	2.00	-3
6300	2.19	2.14	-2
7200	2.31	2.27	-2
9000	2.49	2.48	0
10800	2.71	2.67	-2

**Table 69.** Percentage error of measured and predicted (using NIR PLS model number 8, in section 8.2.4, Table 11) concentrations of butyl acetate for standard reaction number 8 at 50 °C (see thesis section 8.2.2, Table 8), carried out in the 10 L CoFlux® reactor. Butanol addition started at zero seconds.

Time (seconds)	Butyl acetate concentration (moles dm-3) for reaction 8, at 50 °C		Error as a % of butyl acetate concentration
	Measured	PLS model number 8 prediction	
-300	0.00	0.08	-
0	0.00	0.07	-
300	0.57	0.69	20
600	1.03	1.10	8
900	1.32	1.33	1
1200	1.55	1.61	4
1500	1.86	1.87	1
1800	2.05	2.08	1
2400	2.33	2.41	3
3000	2.56	2.65	4
3600	2.81	2.86	2
4500	2.98	3.10	4
5400	3.30	3.30	0
6300	3.43	3.46	1
7200	3.59	3.60	0
9000	3.78	3.81	1
10800	3.96	3.97	0

**Table 70.** Percentage error of measured and predicted (using NIR PLS model number 9, in section 8.2.4, Table 11) concentrations of butyl acetate for the temperature fault reaction number 10 at 40 °C (see thesis section 8.2.2, Table 8), carried out in the 10 L CoFlux® reactor. Butanol addition started at zero seconds.

Time (seconds)	Butyl acetate concentration (moles dm-3) for temperature fault reaction 10		Error as a % of butyl acetate concentration
	Measured	PLS model number 9 prediction	
-300	0.00	0.11	-
0	0.00	0.09	-
300	0.56	0.67	20
600	0.98	1.09	11
900	1.23	1.33	8
1200	1.46	1.58	8
1500	1.80	1.84	2
1800	2.06	2.05	0
2400	2.29	2.36	3
3000	2.47	2.51	2
3600	2.62	2.63	0
4500	2.78	2.80	1
5400	2.83	2.94	4
6300	3.14	3.06	-2
7200	3.21	3.17	-1
9000	3.54	3.36	-5
10800	3.42	3.51	2

**Table 71.** Percentage error of measured and predicted (using NIR PLS model number 10, in section 8.2.4, Table 11) concentrations of butyl acetate for reaction number 11 under fault conditions (see thesis section 8.2.2, Table 8), carried out in the 10 L CoFlux® reactor. Butanol addition started at zero seconds. For the fault reaction 1 % w/w water was added to butanol. Butanol addition started at zero seconds.

Time (seconds)	Butyl acetate concentration (moles dm-3) for fault reaction 11 (1 % water: 99% butanol)		Error as a % of butyl acetate concentration
	Measured	PLS model number 10 prediction	
-300	0.00	-0.01	-
0	0.00	-0.01	-
300	0.48	0.45	-7
600	0.75	0.80	7
900	0.96	1.01	5
1200	1.16	1.22	5
1500	1.38	1.43	4
1800	1.52	1.60	5
2400	1.80	1.88	5
3000	2.05	2.11	3
3600	2.19	2.29	5
4500	2.47	2.53	2
5400	2.62	2.72	4
6300	2.78	2.88	4
7200	2.92	3.02	3
9000	3.20	3.26	2
10800	3.38	3.44	2

**Table 72.** Percentage error of measured and predicted (using NIR PLS model number 11, in section 8.2.4, Table 11) concentrations of butyl acetate for reaction number 12 under fault conditions (see thesis section 8.2.2, Table 8), carried out in the 10 L CoFlux® reactor. Butanol addition started at zero seconds. For the fault reaction 50 % of the TMG volume (97.8 ml) was added at the start of the reaction. Butanol addition started at zero seconds.

Time (seconds)	Butyl acetate concentration (moles dm-3) for TMG fault reaction 12 (50 % TMG)		Error as a % of butyl acetate concentration
	Measured	PLS model number 11 prediction	
-300	0.00	-0.06	-
0	0.00	-0.16	-
300	0.00	0.18	-
600	0.43	0.39	-9
900	0.55	0.53	-3
1200	0.69	0.71	3
1500	0.88	0.88	0
1800	1.02	1.03	1
2400	1.25	1.27	2
3000	1.45	1.48	2
3600	1.64	1.65	1
4500	1.87	1.88	1
5400	1.96	2.07	6
6300	2.19	2.24	2
7200	2.34	2.39	2
9000	2.53	2.65	5
10800	2.97	2.87	-3

**Table 73.** Percentage error of measured and predicted (using NIR PLS model number 12, in section 8.2.4, Table 11) concentrations of butyl acetate for reaction number 13 under fault conditions (see thesis section 8.2.2, Table 8), carried out in the 10 L CoFlux® reactor. Butanol addition started at zero seconds. For the fault reaction the TMG volume changed from 97.8 ml to 195.5 ml at 2100 s. Butanol addition started at zero seconds.

Time (seconds)	Butyl acetate concentration (moles dm-3) for TMG fault reaction 13		Error as a % of butyl acetate concentration
	Measured	PLS model number 12 prediction	
-300	0.00	-0.43	-
0	0.00	-0.17	-
300	0.01	0.18	-
600	0.44	0.40	-10
900	0.56	0.53	-4
1200	0.81	0.72	-11
1500	0.83	0.89	6
1800	1.05	1.03	-2
2400	1.35	1.49	10
3000	1.76	1.84	4
3600	1.92	2.09	9
4500	2.13	2.39	12
5400	2.35	2.62	12
6300	2.61	2.80	8
7200	2.79	2.97	6
9000	3.06	3.22	5
10800	3.31	3.42	3

## 17.7 Prediction of butyl acetate concentrations from MIR PLS models

**Table 74.** Percentage error of measured and predicted (using MIR PLS model number 1, in section 8.2.4, Table 12) concentrations of butyl acetate for standard reaction number 2 at 40 °C (see thesis section 8.2.2, Table 8), carried out in the 10 L CoFlux® reactor. Butanol addition started at zero seconds.

Time (seconds)	Butyl acetate concentration (moles dm-3) for standard reaction 2, at 40 °C		Error as a % of butyl acetate concentration
	Measured	PLS model number 1 prediction	
-300	0.00	0.10	-
0	0.00	0.18	-
300	0.43	0.45	5
600	0.75	0.75	0
900	0.95	1.02	8
1200	1.14	1.21	6
1500	1.34	1.38	3
1800	1.54	1.56	1
2400	1.79	1.82	2
3000	2.03	2.04	1
3600	2.21	2.17	-2
4500	2.48	2.41	-3
5400	2.65	2.57	-3
6300	2.80	2.77	-1
7200	3.02	2.85	-6
9000	3.21	3.05	-5
10800	3.36	3.25	-3

**Table 75.** Percentage error of measured and predicted (using MIR PLS model number 2, in section 8.2.4, Table 12) concentrations of butyl acetate for standard reaction number 3 at 40 °C (see thesis section 8.2.2, Table 8), carried out in the 10 L CoFlux® reactor. Butanol addition started at zero seconds.

Time (seconds)	Butyl acetate concentration (moles dm-3) for standard reaction 3, at 40 °C		Error as a % of butyl acetate concentration
	Measured	PLS model number 2 prediction	
-300	0.00	0.56	-
0	0.00	-0.08	-
300	0.40	0.32	-19
600	0.74	0.71	-5
900	0.97	0.93	-4
1200	1.13	1.13	0
1500	1.38	1.35	-2
1800	1.56	1.62	4
2400	1.81	1.87	3
3000	2.06	2.11	3
3600	2.27	2.29	1
4500	2.43	2.45	1
5400	2.70	2.71	0
6300	2.77	2.79	1
7200	2.86	2.94	3
9000	3.16	3.20	1
10800	3.39	3.42	1

**Table 76.** Percentage error of measured and predicted (using MIR PLS model number 3, in section 8.2.4, Table 12) concentrations of butyl acetate for standard reaction number 4 at 40 °C (see thesis section 8.2.2, Table 8), carried out in the 10 L CoFlux® reactor. Butanol addition started at zero seconds.

Time (seconds)	Butyl acetate concentration (moles dm-3) for standard reaction 4, at 40 °C		Error as a % of butyl acetate concentration
	Measured	PLS model number 3 prediction	
-300	0.00	0.02	-
0	0.00	0.00	-
300	0.38	0.41	10
600	0.80	0.80	1
900	0.97	1.11	14
1200	1.25	1.30	4
1500	1.40	1.53	10
1800	1.54	1.70	10
2400	1.88	1.98	5
3000	2.06	2.21	7
3600	2.22	2.35	6
4500	2.50	2.57	3
5400	2.65	2.79	5
6300	2.84	3.00	6
7200	2.96	3.07	4
9000	3.20	3.30	3
10800	3.33	3.49	5

**Table 77.** Percentage error of measured and predicted (using MIR PLS model number 4, in section 8.2.4, Table 12) concentrations of butyl acetate for standard reaction number 5 at 40 °C (see thesis section 8.2.2, Table 8), carried out in the 10 L CoFlux® reactor. Butanol addition started at zero seconds.

Time (seconds)	Butyl acetate concentration (moles dm-3) for standard reaction 5, at 40 °C		Error as a % of butyl acetate concentration
	Measured	PLS model number 4 prediction	
-300	0.00	-0.06	-
0	0.00	-0.02	-
300	0.49	0.25	-49
600	0.83	0.57	-31
900	1.06	0.88	-17
1200	1.26	1.14	-9
1500	1.39	1.40	1
1800	1.60	1.54	-4
2400	1.96	1.80	-8
3000	2.11	2.04	-3
3600	2.25	2.25	0
4500	2.42	2.46	2
5400	2.72	2.65	-2
6300	2.89	2.79	-3
7200	2.97	2.94	-1
9000	3.34	3.17	-5
10800	3.37	3.37	0

**Table 78.** Percentage error of measured and predicted (using MIR PLS model number 5, section 8.2.4, Table 12) concentrations of butyl acetate for standard reaction number 6, at 40 °C with an increased butanol feed rate, refer to section 8.2.2, Table 8, carried out in the 10 L CoFlux® reactor. Butanol addition started at zero seconds.

Time (seconds)	Butyl acetate concentration (moles dm-3) for reaction 6, with an increased butanol feed rate		Error as a % of butyl acetate concentration
	Measured	PLS model number 5 prediction	
-300	0.00	-0.02	-
0	0.00	0.07	-
300	-	0.41	-
600	0.85	0.80	-7
900	1.19	1.13	-5
1200	1.44	1.37	-5
1500	1.72	1.55	-10
1800	1.74	1.73	0
2400	2.09	1.98	-5
3000	2.16	2.21	2
3600	2.27	2.37	4
4500	2.50	2.58	3
5400	2.63	2.75	4
6300	2.85	2.95	4
7200	2.85	3.04	7
9000	3.14	3.26	4
10800	3.26	3.43	5

**Table 79.** Percentage error of measured and predicted (using MIR PLS model number 6, in section 8.2.4, Table 12) concentrations of butyl acetate for standard reaction number 7, at 30 °C, refer to section 8.2.2, Table 8, carried out in the 10 L CoFlux® reactor. Butanol addition started at zero seconds.

Time (seconds)	Butyl acetate concentration (moles dm-3) for reaction 7, at 30 °C		Error as a % of butyl acetate concentration
	Measured	PLS model number 6 prediction	
-300	0.00	-0.02	-
0	0.00	0.07	-
300	0.31	0.22	-30
600	0.56	0.51	-8
900	0.74	0.75	2
1200	0.87	0.91	5
1500	1.06	1.08	2
1800	1.16	1.23	7
2400	1.34	1.46	9
3000	1.51	1.64	9
3600	1.76	1.81	3
4500	1.88	2.02	7
5400	2.05	2.14	5
6300	2.19	2.30	5
7200	2.31	2.45	6
9000	2.49	2.62	5
10800	2.71	2.83	4

**Table 80.** Percentage error of measured and predicted (using MIR PLS model number , in section 8.2.4, Table 12) concentrations of butyl acetate for standard reaction number 7, at 50 °C, refer to section 8.2.2, Table 8, carried out in the 10 L CoFlux® reactor. Butanol addition started at zero seconds.

Time (seconds)	Butyl acetate concentration (moles dm-3) for reaction 8, at 50 °C		Error as a % of butyl acetate concentration
	Measured	PLS model number 7 prediction	
-300	0.00	0.02	-
0	0.00	0.05	-
300	0.57	0.50	-13
600	1.03	0.94	-8
900	1.32	1.28	-3
1200	1.55	1.55	0
1500	1.86	1.85	0
1800	2.05	2.04	-1
2400	2.33	2.34	0
3000	2.56	2.58	1
3600	2.81	2.78	-1
4500	2.98	3.04	2
5400	3.30	3.23	-2
6300	3.43	3.36	-2
7200	3.59	3.52	-2
9000	3.78	3.69	-2
10800	3.96	3.86	-3

**Table 81.** Percentage error of measured and predicted (using MIR PLS model number , in section 8.2.4, Table 12) concentrations of butyl acetate for reaction number 10, with a purposefully introduced temperature fault, refer to section 8.2.2, Table 8, carried out in the 10 L CoFlux® reactor. Butanol addition started at zero seconds.

Time (seconds)	Butyl acetate concentration (moles dm-3) for temperature fault reaction 10		Error as a % of butyl acetate concentration
	Measured	PLS model number 8 prediction	
-300	0.00	-0.13	-
0	0.00	-0.13	-
300	0.56	0.43	-24
600	0.98	0.84	-15
900	1.23	1.18	-4
1200	1.46	1.49	2
1500	1.80	1.73	-4
1800	2.06	1.93	-6
2400	2.29	2.27	-1
3000	2.47	2.46	0
3600	2.62	2.56	-2
4500	2.78	2.72	-2
5400	2.83	2.87	2
6300	3.14	2.99	-5
7200	3.21	3.11	-3
9000	3.54	3.30	-7
10800	3.42	3.45	1

**Table 82.** Percentage error of measured and predicted (using MIR PLS model number, in section 8.2.4, Table 12) concentrations of butyl acetate for reaction number 11, under fault conditions, see thesis section 8.2.2, Table 8, carried out in the 10 L CoFlux® reactor. For the fault reaction 1 % w/w water was added to butanol. Butanol addition started at zero seconds.

Time (seconds)	Butyl acetate concentration (moles dm-3) for fault reaction 11 (1 % water: 99% butanol)		Error as a % of butyl acetate concentration
	Measured	PLS model number 9 prediction	
-300	0.00	-0.05	-
0	0.00	-0.07	-
300	0.48	0.33	-32
600	0.75	0.64	-15
900	0.96	0.94	-2
1200	1.16	1.20	4
1500	1.38	1.40	2
1800	1.52	1.57	3
2400	1.80	1.90	5
3000	2.05	2.09	2
3600	2.19	2.31	5
4500	2.47	2.53	2
5400	2.62	2.72	4
6300	2.78	2.88	4
7200	2.92	3.02	3
9000	3.20	3.22	1
10800	3.38	3.43	2